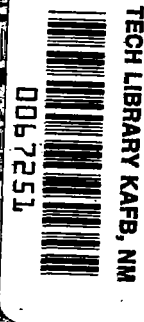NASA
CCF
PR-4
c.1

NASA CONTRACTOR REPORT

NASA CR-2711

CARBIDE COATED FIBERS IN GRAPHITE-ALUMINUM COMPOSITES

Progress Report No. 4: January 1 - June 30, 1975

Richard J. Imprescia, Leonard S. Levinson,
Robert D. Reiswig, Terry C. Wallace,
and Joel M. Williams

Prepared by
LOS ALAMOS SCIENTIFIC LABORATORY
Los Alamos, N.M. 87544
for Langley Research Center

NATIONAL AERONAUTICS AND SPACE ADMINISTRATION • WASHINGTON, D. C. • JULY 1976

0067251

1. Report No. NASA CR-2711	2. Government Accession No.	3. Recipient's Catalog No.
4. Title and Subtitle CARBIDE COATED FIBERS IN GRAPHITE-ALUMINUM COMPOSITES Progress Report No. 4: January 1 - June 30, 1975		5. Report Date July 1976
		6. Performing Organization Code
7. Author(s) Richard J. Imprescia, Leonard S. Levinson, Robert D. Reiswig, Terry C. Wallace, Joel M. Williams		8. Performing Organization Report No. LA-6181-PR
		10. Work Unit No.
9. Performing Organization Name and Address Los Alamos Scientific Laboratory Los Alamos, NM 87544		506-16-21-01
		11. Contract or Grant No. L75,900
		13. Type of Report and Period Covered
12. Sponsoring Agency Name and Address National Aeronautics and Space Administration Washington, DC 20546		Contractor Report
		14. Sponsoring Agency Code

15. Supplementary Notes
This is the last progress report on this research program. Previous reports on this research are: NASA CR-2533, NASA CR-2566, and NASA CR-2601. Dennis L. Dicus was technical monitor for NASA Langley Research Center.

16. Abstract
This report describes the fourth and final part of an NASA-supported program at the Los Alamos Scientific Laboratory to develop graphite fiber-aluminum matrix composites. A chemical vapor deposition apparatus was constructed for continuously coating graphite fibers with TiC. As much as 150 metres of·continuously coated fibers were produced. Deposition temperatures were varied from 1365 K to about 1750 K, and deposition time from 6 to 150 seconds. The 6 sec deposition time corresponded to a fiber feed rate of 2.54 m/min through the coater. Thin, uniform, adherent TiC coats, with thicknesses up to approximately 0.1 µm, were produced on the individual fibers of Thornel 50 graphite yarns without affecting fiber strength. Although coat properties were fairly uniform throughout a given batch, more work is needed to improve the batch-to-batch reproducibility.
   Samples of TiC-coated Thornel 50 fibers were infiltrated with an aluminum alloy and hot-pressed in vacuum to produce small composite bars for flexure testing. Strengths as high as 90% of the rule-of-mixtures strength were achieved. Examination of the fracture surfaces indicated that the bonding between the aluminum and the TiC-coated fibers was better than that achieved in a similar, commercially infiltrated material made with fibers having no observable surface coats.
   Several samples of Al-infiltrated, TiC-coated Thornel 50 graphite yarns, together with samples of the commercially infiltrated, uncoated fibers, were heated for 100 hours at temperatures near the alloy solidus. The TiC-coated samples appeared to undergo less reaction than did the uncoated samples.

Subject Category 24 Composite Materials

17. Key Words (Suggested by Author(s)) Graphite-aluminum composites, Graphite fibers, Chemical vapor deposition, Aluminum alloy matrix, Liquid metal infiltration, Titanium carbide coating, Diffusion barrier coating	18. Distribution Statement Unclassified-Unlimited Subject Category 24

19. Security Classif. (of this report) Unclassified	20. Security Classif. (of this page) Unclassified	21. No. of Pages 41	22. Price* $3.75

*For sale by the National Technical Information Service, Springfield, Virginia 22161

CARBIDE COATED FIBERS IN GRAPHITE-ALUMINUM COMPOSITES

Progress Report No. 4

January 1 - June 30, 1975

By Richard J. Imprescia, Leonard S. Levinson, Robert D. Reiswig,
Terry C. Wallace, and Joel M. Williams

SUMMARY

A chemical vapor deposition apparatus was constructed for continuously
coating graphite fibers with TiC. As much as 150 metres of continuously coated
fibers were produced. Deposition temperatures were varied from 1365 K to about
1750 K, and deposition time from 6 to 150 sec. The 6 sec deposition time cor-
responded to a fiber feed rate of 2.54 m/min through the coater. Thin, uniform,
adherent TiC coats, with thicknesses up to approximately 0.1 μm, were produced
on the individual fibers of Thornel 50 graphite yarns without affecting fiber
strength. Although coat properties were fairly uniform throughout a given batch,
more work is needed to improve the batch-to-batch reproducibility.

Samples of TiC-coated Thornel 50 fibers were infiltrated with an aluminum
alloy and hot-pressed in vacuum to produce small composite bars for flexure tes-
ting. Strengths as high as 90% of the rule-of-mixtures strength were achieved.
Examination of the fracture surfaces indicated that the bonding between the alu-
minum and the TiC-coated fibers was better than that achieved in a similar, com-
mercially infiltrated material made with fibers having no observable surface
coats.

Several samples of Al-infiltrated, TiC-coated Thornel 50 graphite yarns, to-
gether with samples of the commercially infiltrated, uncoated fibers, were heated
for 100 h at temperatures near the alloy solidus. The TiC-coated samples appeared
to undergo less reaction than did the uncoated samples.

INTRODUCTION

The work described here is the final phase of a NASA-supported program at
the Los Alamos Scientific Laboratory (LASL) to develop graphite fiber-aluminum
matrix composites. The LASL approach to this problem has been to use protective-
coupling layers of refractory metal carbides on the graphite fibers prior to
their incorporation into the composites. It was thought that such layers would
be directly wettable by liquid aluminum and should act as diffusion barriers to
inhibit reaction between graphite fibers and liquid aluminum.[1]

In the earlier phases of this program,[1,2,3] chemical vapor deposition (CVD)
methods were developed for producing thin, uniform, coats of ZrC and TiC on gra-
phite fibers, using a batch process. Attempts were also made to produce SiC
coats, but with only limited success. Successful wetting and infiltration of
TiC-coated graphite fibers with aluminum alloys was demonstrated, and moderate

success was achieved in producing small graphite–aluminum composite samples by vacuum hot–pressing of aluminum–infiltrated graphite yarns. Thin TiC coats on graphite fibers were shown to inhibit the reaction between the fibers and aluminum at elevated temperatures.

In the batch coating operation used earlier, the fiber samples were limited to lengths of about 150 mm. Therefore, to demonstrate the practicality of the coating process it was desired to construct an apparatus for continuously coating fibers in much longer lengths. Such an apparatus was constructed and was used successfully to produce TiC–coated fibers in continuous lengths up to 150 metres. The apparatus and its use are described here.

Techniques were also developed for compacting Al–infiltrated, TiC–coated fibers into small composite bars suitable for testing mechanical properties. The forming process and the composite properties are given.

EXPERIMENTAL

Continuous Coating

A schematic of the continuous coating system is shown in Fig. 1, and a more detailed description of its components and operation is given in APPENDIX A. For the experiments described here, this apparatus was used to produce TiC coats on graphite fibers, using purified, commercial grade $TiCl_4$ as the coating gas.
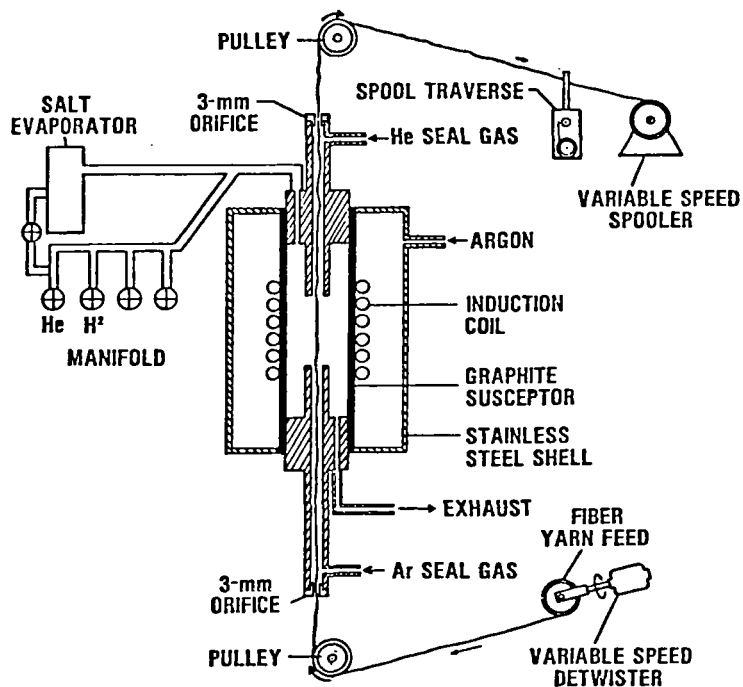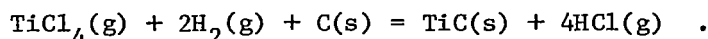

Fig. 1. Schematic of system for continuous coating of graphite fibers.

The basic chemical reaction controlling the decomposition of $TiCl_4$, leading to the formation of TiC on graphite fibers, is:

$$TiCl_4(g) + 2H_2(g) + C(s) = TiC(s) + 4HCl(g) \quad .$$

The carbon necessary for the reaction is provided by the fiber substrate. Besides the coating gases, helium is added as a diluent, together with excess hydrogen. The deposition kinetics can be varied by varying the deposition temperature and the proportions of the gases.

Continuous coating of graphite fibers with TiC was performed under nearly 80 different sets of process conditions. The fibers used for the experiments were two-ply (720 fibers/ply), Thornel 50 graphite yarns, obtained from Union Carbide Corporation. The coating conditions are listed in Table I, together with the results of scanning electron microscopy (SEM) observations of the coat characteristics, TiC coat thicknesses, and strengths (tensile breaking loads) of the fiber yarns. The method for determining the fiber yarn strengths is given in APPENDIX B. Table I also includes the data for three lots of batch-coated fibers that were used in experiments to be described later.

The coat thickness values reported in Table I are averages of from 10 to 15 measurements made on SEM photomicrographs of polished cross sections of epoxy-mounted samples. These were made with a millimeter scale on from three to five fiber cross sections. The magnification of the photomicrographs was usually 10,000X. At this magnification a coat thickness of 0.1 μm would be magnified to 1 mm. With a millimeter scale it is possible to estimate a length of about 0.2 mm, which corresponds to 0.02 μm, magnified 10,000 times. Therefore, the measurements from which the average coat-thickness values of Table I were computed have an uncertainty of at least 0.02 μm. This uncertainty, together with coat thickness variations, has led to rather high standard deviations of the mean values. This is particularly true for samples with very thin coats (e.g., runs 8AA-8TT).

Although the thickness values were determined from relatively few samples from each run, the coat appearances were determined by SEM examination of several hundred fibers from each run. As indicated in Table I, a variety of TiC coat morphologies was observed in these experiments. SEM photomicrographs representing typical examples of this variety are given in APPENDIX C.

In the initial runs (1A through 3J) virtually all of the TiC coats underwent some oxidation. This was evidenced, generally, by a blue or green cast on the surfaces of the TiC-coated fibers (Table I), and sometimes by a loose, white, powdery deposit, which was probably hydrated TiO_2. Typical samples with each of the predominant colors were examined by x-ray diffraction, which showed that both the blue and green colors were caused by the presence of the rutile form of TiO_2. Those samples with a heavy blue cast were shown by x-ray intensity measurements to have coats consisting of nearly as much rutile as TiC. This observation was supported by microscopic observations which showed such coats to consist of mixed phases of two different structures, apparently codeposited. The samples having a green cast similarly were shown to consist of the same two phases, but with a much lower concentration of rutile. It was discovered that at least part of the problem causing this oxidation was impure hydrogen in the coating gas mixture. This was rectified by installation of

TABLE I

COATING CONDITIONS AND RESULTS FOR TiC-COATED THORNEL 50 YARNS

Run No.	Fiber Feed Rate, m/min	Deposition: Temp, K	Deposition: Time, sec	Coating Gases ℓ(STP)/min TiCl$_4$	H$_2$	He[a]	Coat Appearance (SEM)	Coat Thickness, μm mean	std dev	CV[b]	Tensile Breaking Load,[c] N mean	std dev	CV[b]
1A	0.13	1493	110	0.44	5	10	rough, v. few cracks,[d] few welds, blue-gray	---	---	---	28.45	2.89	0.10
1B	0.13	1761	110	0.44	5	10	v. rough, spalls, cracks, many welds	0.85	0.21	0.25	7.75	0.91	0.12
1C	1.40	1761	11	0.44	5	10	rough, v. few cracks, few welds, blue	---	---	---	24.05	2.00	0.08
2A	0.11	1486	135	0.19	5	10	rough, nodules, v. few cracks, few welds, whitish	---	---	---	24.44	2.00	0.08
2B	0.11	1628	135	0.19	5	10	rough, nodules, v. few cracks, few welds, green	---	---	---	11.56	2.18	0.19
2C	0.33	1628	46	0.19	5	10	rough, v. few welds, blue-green	0.10	0.01	0.11	19.98	1.69	0.08
2D	0.51	1628	30	0.19	5	10	rough, few welds, green	---	---	---	20.09	1.51	0.08
2E	0.64	1628	24	0.19	5	10	rough, few nodules, few cracks, green	---	---	---	22.06	2.22	0.10
2F	0.76	1628	20	0.19	5	10	smooth, v. few welds, blue-green	0.09	0.02	0.20	21.00	1.89	0.09
2G	1.40	1628	11	0.19	5	10	smooth, nodules, v. few cracks, blue	0.10	0.02	0.25	21.60	0.92	0.04
2H	0.76	1522	20	0.19	5	10	smooth, v. few nodules, blue-green	0.09	0.01	0.15	24.98	2.98	0.12
2I	0.76	1425	20	0.19	5	10	smooth, few nodules, few welds, green	0.09	0.02	0.22	25.78	2.34	0.09
2J	0.76	1324	20	0.19	5	10	smooth, many nodules, v. few cr., few welds, blue-white	---	---	---	23.93	2.03	0.08
3A	0.76	1625	20	0.04	5	10	smooth, few nodules, v. few cr., few welds, blue	---	---	---	25.03	2.00	0.08
3B	0.76	1512	20	0.04	5	10	smooth, few nodules, few welds, blue	0.09	0.03	0.29	26.02	2.32	0.09
3C	0.76	1425	20	0.04	5	10	rough, nonunif.[e] nodules , few welds, whitish	---	---	---	26.93	1.24	0.05
3D	0.51	1414	20	0.04	5	10	smooth, nonunif.[e] v. few nodules, blue-green	---	---	---	26.60	1.64	0.06
3E	0.25	1422	60	0.04	5	10	smooth, few nodules, few welds, green	0.09	0.02	0.21	27.72	1.73	0.06
3F	0.25	1469	60	0.04	5	10	smooth, few nodules, few welds, blue-white	---	---	---	27.36	1.23	0.05
3G	0.25	1672	60	0.04	5	10	rough, v. few nodules, few welds, gold-gray	---	---	---	23.06	1.78	0.08
3H	0.51	1681	30	0.04	5	10	rough, nodules, sl. blue	---	---	---	23.60	1.16	0.04
3I	0.76	1684	20	0.04	5	10	rough, nodules, few welds, sl. blue	0.08	0.02	0.27	24.48	1.42	0.06
3J	0.76	1686	20	0.11	5	10	rough, nodules, few welds, sl. blue	---	---	---	14.02	2.15	0.15
4D	0.76	1588	20	0.17	9	12	sl. rough, few nodules, few welds	0.21	0.04	0.21	19.27	1.89	0.10
4E	1.40	1588	11	0.17	9	12	smooth, few nodules, v. few cracks, few welds	0.20	0.04	0.21	24.20	1.65	0.07
4F	1.40	1743	11	0.17	9	12	rough, v. few cracks, few welds	0.32	0.10	0.30	5.73	1.24	0.22
4G	2.54	1743	6	0.17	9	12	smooth, few nodules, many cracks, few welds	0.25	0.06	0.23	16.03	1.86	0.12
4H	2.54	1628	6	0.17	9	12	sl. rough, v. few cracks, few welds	0.18	0.04	0.20	21.57	1.78	0.08
5A	2.54	1747	6	0.12	9	12	smooth, many cracks, few welds, spalls	0.18	0.03	0.15	19.25	1.30	0.07
5B	2.54	1747	6	0.27	9	12	smooth, many cracks, spalls	0.20	0.03	0.13	14.22	0.59	0.04
5C	2.54	1668	6	0.27	9	12	smooth, few cracks, few welds	0.13	0.04	0.31	16.34	1.47	0.09
5D	1.65	1668	9	0.27	9	12	smooth, many cracks, few welds	---	---	---	15.53	1.87	0.12
5E	2.54	1668	6	0.60	9	12	rough, v. few cracks, few welds	0.13	0.04	0.30	16.10	1.46	0.09

TABLE I (Continued)

Run No.	Fiber Feed Rate, m/min	Deposition: Temp, K	Deposition: Time, sec	Coating Gases ℓ(STP)/min TiCl$_4$	H$_2$	He[a]	Coat Appearance (SEM)	Coat Thickness, μm mean	std dev	CV[b]	Tensile Breaking Load,[c] N mean	std dev	CV[b]
5F	1.65	1668	9	0.60	9	12	smooth, few nodules, few cracks, few welds	---	---	---	13.97	1.56	0.11
5G	2.54	1668	6	0.05	9	12	smooth, nonuniform[e], many cracks, few welds, spalls.	---	---	---	21.20	2.28	0.11
5H	1.65	1668	9	0.05	9	12	rough, few cracks, few welds	0.12	0.03	0.30	21.36	1.51	0.07
5I	1.65	1567	9	0.67	9	12	smooth, v. few cracks, few welds	0.09	0.03	0.38	22.15	1.54	0.07
5J	2.54	1567	6	0.67	9	12	smooth, v. few cracks, few welds	0.09	0.02	0.26	21.23	2.03	0.10
5K	2.54	1567	6	0.16	9	12	smooth, few nodules, v. few cracks, few welds	0.09	0.02	0.19	20.82	1.73	0.08
5L	1.65	1567	9	0.16	9	12	smooth, few nodules, v. few cracks, few welds	0.11	0.03	0.29	19.56	1.42	0.07
5M	1.65	1567	9	0.04	9	12	smooth, few nodules, v. few cracks, few welds	0.08	0.02	0.22	23.01	1.49	0.06
5N	2.54	1567	6	0.04	9	12	smooth, nonunif.,[e] few nodules, v. few cracks, few welds	0.08	0.05	0.60	22.29	2.05	0.09
5O	2.54	1468	6	0.04	9	12	smooth, v. nonunif.,[f] few nodules, v. few cracks	0.07	0.03	0.37	22.66	0.87	0.04
5P	1.65	1468	9	0.04	9	12	smooth, v. nonunif.,[f] few nodules, v. few cracks	0.06	0.04	0.64	22.78	1.48	0.06
5R	1.65	1468	9	0.09	9	12	smooth, v. nonunif.,[f] few nodules, v. few cracks	---	---	---	23.84	1.38	0.06
5S	2.54	1468	6	0.09	9	12	smooth, v. nonunif.,[f] few nodules, v. few cracks	---	---	---	22.13	2.37	0.11
5T	2.54	1468	6	0.74	9	12	smooth, v. nonunif.,[f] few nodules, v. few cracks	0.08	0.05	0.62	21.64	0.95	0.04
5U	1.65	1468	9	0.74	9	12	smooth, v. nonunif.,[f] few nodules, v. few cracks	---	---	---	21.35	2.09	0.09
8AA	0.76	1524	20	0.02	12	11	smooth, v. nonunif.,[f] few nodules, many welds	---	---	---	11.35	0.67	0.06
8BB	2.54	1524	6	0.02	12	11	smooth, v. nonunif.,[f] few nodules	---	---	---	20.34	0.86	0.04
8CC	2.54	1524	6	0.02	12	11	smooth, v. nonunif.,[f] few nodules	---	---	---	19.59	1.05	0.05
8DD	2.54	1582	6	0.02	12	11	smooth, few nodules	0.04	0.05	1.0	19.19	1.05	0.05
8EE	2.54	1582	6	0.02	12	11	smooth, few nodules	0.04	0.03	0.87	19.01	1.53	0.08
8FF	0.76	1582	20	0.02	12	11	smooth, v. nonunif.,[f] few nodules, many welds	0.07	0.04	0.62	6.60	0.61	0.09
8GG	1.65	1582	9	0.02	12	11	smooth, v. nonunif.,[f] few nodules, many welds	0.07	0.06	0.85	12.00	0.93	0.08
8HH	0.76	1489	20	0.02	12	11	smooth, v. nonunif.,[f] few nodules, many welds	---	---	---	9.65	1.36	0.14
8II	1.65	1489	9	0.02	12	11	smooth, v. nonunif.,[f] few nodules	---	---	---	18.58	1.51	0.08
8KK	2.54	1489	6	0.02	12	11	smooth, v. nonunif.,[f] few nodules	---	---	---	20.97	1.27	0.06
8LL	0.76	1431	20	0.02	12	11	smooth, v. nonunif.,[f] few nodules, many welds	0.05	0.04	0.72	13.94	1.44	0.10
8MM	1.65	1431	9	0.02	12	11	smooth, v. nonunif.,[f] few nodules, many welds	0.03	0.03	1.2	18.64	1.23	0.07
8NN	1.65	1431	9	0.02	12	11	smooth, few nodules, few welds	0.03	0.03	1.0	20.23	1.02	0.05
8OO	2.54	1431	6	0.02	12	11	smooth, few nodules, few welds	0.04	0.03	1.0	19.37	1.72	0.09
8PP	0.36	1431	43	0.02	12	11	smooth, v. nonunif.,[f] few nodules, many welds	0.07	0.02	0.29	6.85	0.55	0.08
8RR	0.36	1365	43	0.02	12	11	smooth, few nodules, many welds	---	---	---	13.85	1.72	0.12
8SS	0.51	1365	30	0.02	12	11	smooth, nonunif.,[e] few nodules	---	---	---	18.15	1.34	0.07
8TT	0.76	1365	20	0.02	12	11	smooth, v. nonunif.,[f] few nodules	---	---	---	17.59	1.73	0.10

TABLE I (Continued)

Run No.	Fiber Feed Rate, m/min	Deposition: Temp, K	Time, sec	Coating Gases ℓ(STP)/min TiCl$_4$	H$_2$	He[a]	Coat Appearance (SEM)	Coat Thickness, μm mean	std dev	CV[b]	Tensile Breaking Load,[c] N mean	std dev	CV[b]
9A	0.76	1377	20	0.20	14	12	smooth, few nodules	0.07	0.01	0.19	22.39	2.77	0.12
9B	1.65	1377	9	0.20	14	12	smooth	0.04	0.03	0.78	21.30	2.23	0.10
9C	2.54	1377	6	0.20	14	12	smooth, few nodules	0.03	0.03	1.0	22.15	2.12	0.10
9D	0.76	1430	20	0.20	14	12	smooth, few nodules	0.08	0.02	0.26	21.76	2.54	0.12
9E	1.65	1430	9	0.20	14	12	smooth, few nodules	0.05	0.03	0.68	23.29	2.09	0.09
9F	2.54	1430	6	0.20	14	12	smooth, few welds	0.05	0.02	0.42	24.57	1.66	0.07
9G	0.76	1477	20	0.20	14	12	smooth, few welds	0.07	0.02	0.31	24.41	2.56	0.10
9H	1.65	1477	9	0.20	14	12	smooth, v. nonuniform,[f] few welds	0.04	0.04	0.92	23.83	1.64	0.07
9I	2.54	1477	6	0.20	14	12	smooth, v. nonuniform,[f] few welds	0.03	0.02	0.83	23.50	2.20	0.09
9K	2.54	1573	6	0.20	14	12	smooth, v. nonuniform[f]	0.04	0.03	0.80	22.54	1.89	0.08
9L	1.65	1573	9	0.20	14	12	smooth, few nodules, few welds	0.09	0.03	0.30	16.85	1.76	0.10
2-21-75[g]	---	1273	3600	0.24	5	10	smooth, v. nonuniform,[f] nodules	0.03	0.02	0.72	14.75	1.79	0.12
3-17-75[g]	---	1273	3600	0.33	5	10	rough, few nodules	0.09	0.01	0.10	8.94	1.20	0.13
8-14-74[g]	---	1226	3600	0.41	5	10	smooth, few nodules	0.10	0.02	0.17	21.10	1.49	0.07
Control[h]	---	---	---	---	--	--	---	0	---	---	22.38	2.14	0.10

[a] Additional helium was used at the top (fiber exit) gas seal. This varied from 2 to 17 ℓ(STP)/min depending on other run conditions. It is not known how much of this entered the furnace as diluent and how much escaped.

[b] Coefficient of variation (std dev ÷ mean).

[c] Measured on one ply of two-ply yarn.

[d] Primarily transverse cracks. Longitudinal cracks appeared to occur only along with transverse cracks.

[e] Variation in coat thickness on individual fibers.

[f] Thickness varied from outer to inner fibers of the yarn, as well as on individual fibers.

[g] Batch-coated.

[h] Uncoated, as-received, PVA-sized Thornel 50.
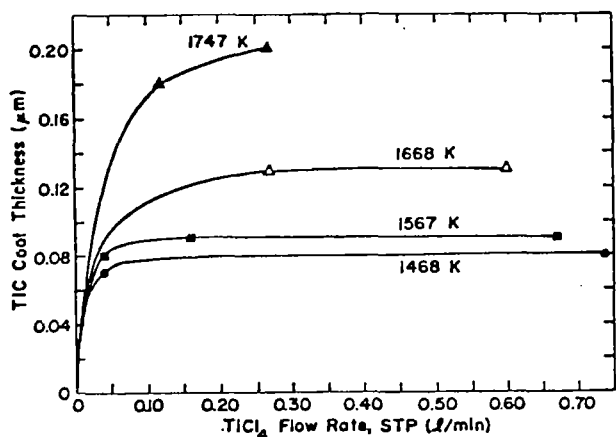
Fig. 2. TiC coat thickness vs flow rate of TiCl$_4$. Coating time = 6 sec (Series No. 5).

a purification system to remove both water and oxygen from the hydrogen. Even after installation of this system, however, it was found that occasionally a blue cast would begin to appear sometime after a coating run was well under way. This was also eliminated by careful regulation of the seal-gas flows at each end of the furnace and of the pressure at the exhaust duct. At the start of each run, the seal-gas flows were adjusted until no trace of blue or green was visible and the fibers emerging from the furnace had the typical, metallic gray color of TiC. However, regardless of the seal gas flows, the pressure on the exhaust line (Fig. 1) had to be maintained at 30 to 50 Pa below atmospheric pressure[*] to prevent fiber oxidation.
During the course of a coating run, agglomerates of broken fibers tended to collect at the fiber exit near the helium gas seal, causing a change in the pressure in the system. This was further complicated by the fact that these fiber agglomerates would occasionally break loose and be pulled from the top of the furnace by the emerging coated fiber. Therefore, particular care was taken to maintain the exhaust pressure at the prescribed level. This was done simply by adjusting a sliding-gate damper on the exhaust duct, and by varying the helium flow rate into the fiber exit gas seal at the top of the furnace. Throughout these experiments it was necessary to vary this helium flow rate from 2 to 17 ℓ(STP)/min to maintain the proper exhaust pressure. By taking these precautions, the remainder of the coating runs gave no visible indication of oxygen contamination in the TiC coats, and x-ray examination of selected samples supported this observation.

Examination of the data of Table I shows that general relationships between the coating conditions and the TiC coat characteristics are not obvious at this time. Within a given coating series, however, there can be good correlations between a coat characteristic and process conditions. For instance, in Fig. 2 the TiC coat thickness is plotted as a function of the coating gas (TiCl$_4$) flow rate for four different deposition temperatures and a 6 sec deposition time. These data are taken from Series No. 5 (runs 5A-5U) in Table I. Although the relationships here are quite clear, the few additional data points from Series No. 8 and No. 9 that could be plotted in this figure do not fall on any of the curves.

Despite this lack of consistency, such data are useful in elucidating the general nature of the process. From Fig. 2, it is seen that the relationship between deposition temperature and coating gas flow rate can be an important

_____

[*]Average atmospheric pressure at the site of these experiments in Los Alamos, NM, is ~77 kPa (580 mm Hg).

consideration in the control of the process. At the two lower temperatures (1468 and 1567 K), it is seen that the coat thickness is constant and independent of the flow rate at values above about 0.1 ℓ(STP)/min $TiCl_4$. Below this point, however, coat thickness changes rapidly with flow rate, and, therefore, is a serious consideration in the control of the deposition process. This behavior is what would be expected in view of the fact that the deposition reaction is a solid state, diffusion-limited process. After the initial reaction of $TiCl_4$ with the graphite fibers, the TiC coat formed acts as a diffusion barrier, which increasingly impedes the reaction as thickness increases, until the reaction becomes undetectably slow and the thickness becomes essentially constant at some maximum value. Because diffusion rates are exponential functions of temperature, the maximum coat thickness increases greatly with temperature, as shown in Fig. 2. The thickness, of course, is also a function of deposition time.

To examine the effect of deposition time on coat characteristics, coating series No. 8 (runs 8AA-8TT) and No. 9 (runs 9A-9L) were made at $TiCl_4$ flow rates of 0.02 ℓ(STP)/min and 0.20 ℓ(STP)/min, respectively, and deposition time was varied from 6 to 43 sec. In general, the TiC coats produced were thin and smooth with few nodular growths. Very little spallation and cracking occurred, indicating that adherence was also good. For Series No. 8, which was produced using 0.02 ℓ(STP)/min $TiCl_4$, welding together of fibers was common, and the coat thickness uniformity for most samples was poor. Not only was the coat thickness nonuniform on individual fibers, but it varied from the outer to the inner fibers of the yarn. On the other hand, Series No. 9, which was produced with 0.20 ℓ(STP)/min $TiCl_4$, had few welds between fibers and significantly better coat thickness uniformity. The data from Table I are graphically shown in Figs. 3 and 4. The coat thickness behavior for both series is similar. Initially, thickness increases rapidly with coating time, then tends to level off at a constant value. For the samples coated at 1582 K, with a $TiCl_4$ flow rate of 0.02 ℓ(STP)/min (Fig. 3), the leveling off occurred at a coating time of about 9 sec and a coat thickness of 0.07 μm. The curve for the samples coated with the higher $TiCl_4$ flow rate (0.20 ℓ/min) and at a similar temperature (1573 K) appears not to have reached the leveling-off point at this coating time (Fig. 4). Neither of the curves for the samples coated at the lower temperature, for Series No. 8 or No. 9, has reached a constant thickness value at the coating times given here. In general, those samples coated at a $TiCl_4$ flow rate of 0.20 ℓ(STP)/min (Fig. 4) have greater TiC coat thicknesses, for equivalent coating times and temperatures, than do those coated at 0.02 ℓ(STP)/min (Fig. 3). Again, the few data points from Series No. 4 and No. 5 that could be plotted in Figs. 3 and 4 do not agree at all with the curves plotted there. Instead they fall at thickness values significantly higher, for the equivalent coating time (6 sec).

In Figs. 5 and 6, the effect of TiC coat thickness on the strength of the fibers is shown. The values given are the tensile breaking loads for single plies of the two-ply yarns. For Series No. 4, 5 and 9 the strength remained fairly constant, relative to the control (zero-thickness) strength, up to thicknesses of about 0.08 μm. For greater thicknesses, strength dropped rapidly for all three series. Series No. 8, however, differed from the others in that strength decreased significantly with even the thinnest coats and dropped to almost insignificant values at a coat thickness of 0.07 μm.

The lack of reproducibility in strength and in coat characteristics, for coats produced under similar conditions, points up the need for further work in
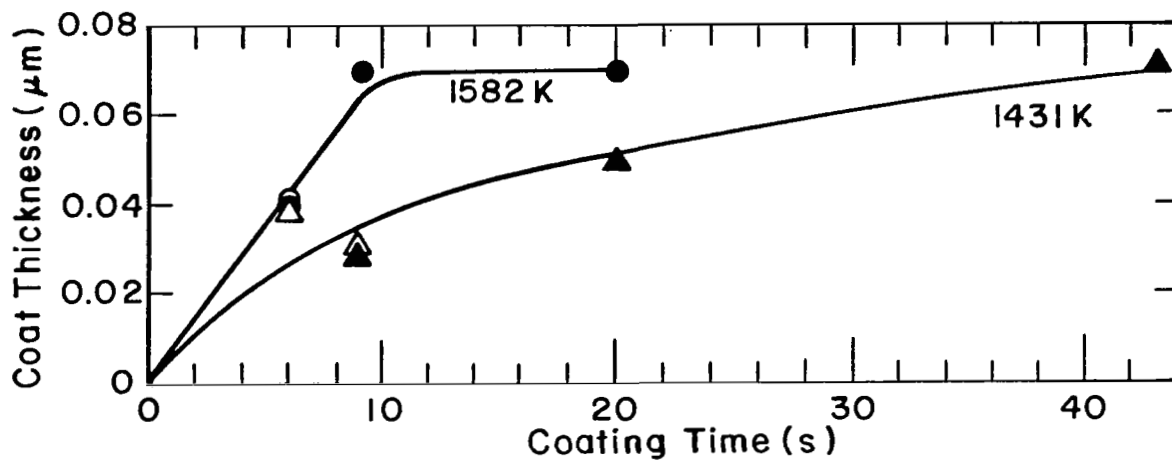
Fig. 3. TiC coat thickness vs coating time. $TiCl_4$ flow rate = 0.02 ℓ(STP)/min (Series No. 8).
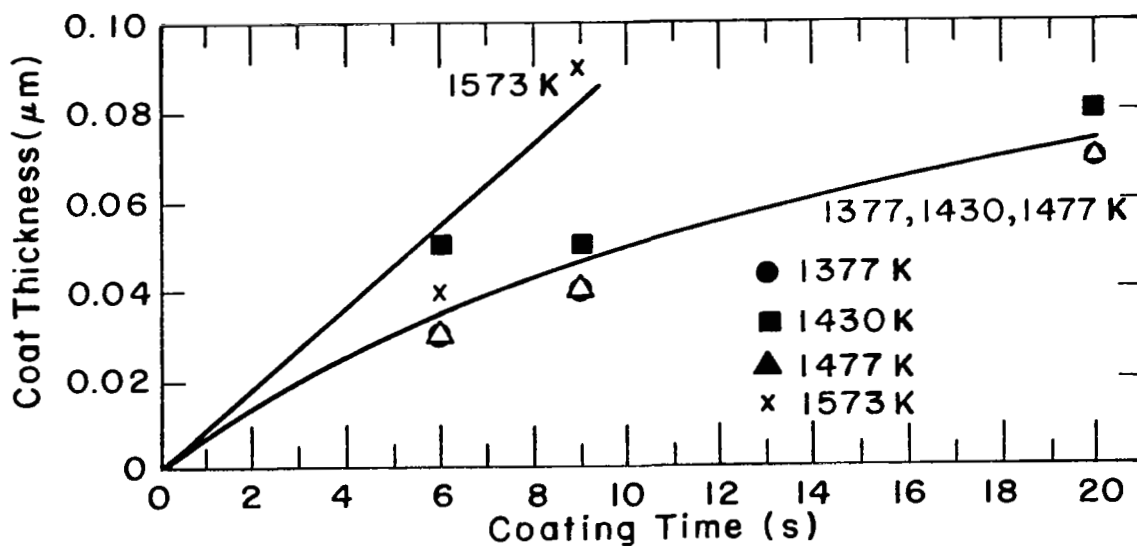

Fig. 4. TiC coat thickness vs coating time. $TiCl_4$ flow rate = 0.20 ℓ(STP/min (Series No. 9).
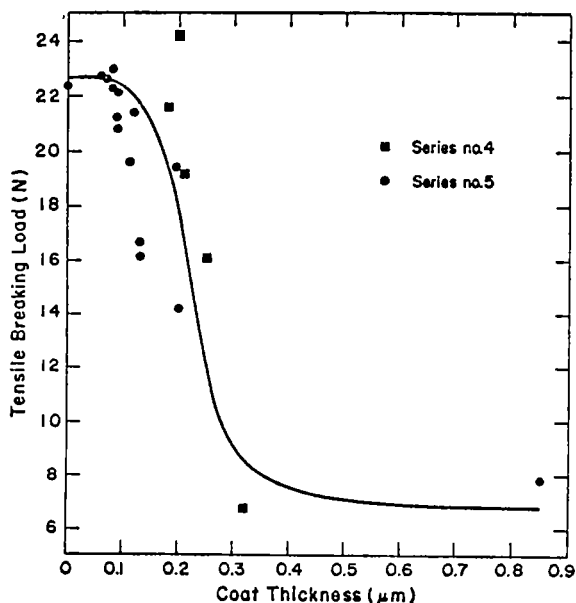
Fig. 5. Tensile breaking load vs coat thickness for TiC-coated Thornel 50 graphite fiber yarns (Series No. 4 and No. 5).
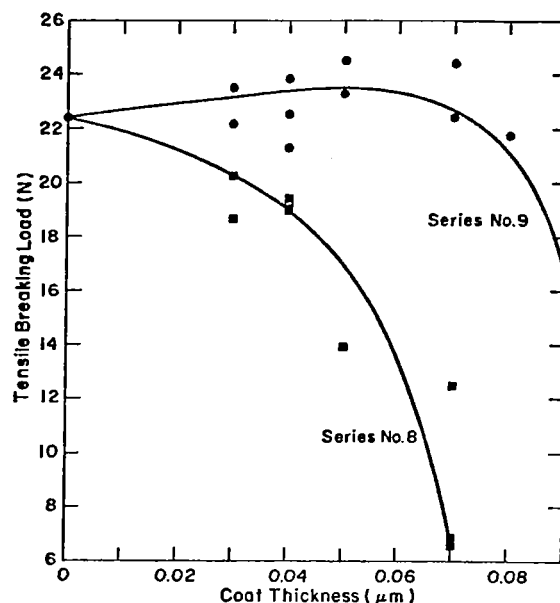
Fig. 6. Tensile breaking load vs coat thickness for TiC-coated Thornel 50 graphite fiber yarns (Series No. 8 and No. 9).

defining the influencing process variables. Obviously, there are process considerations, not apparent here, which are responsible for these variations.

In all of the continuous coating runs described in Table I, the length of yarn coated was about 15 metres. To evaluate the uniformity in TiC coat properties over longer lengths of continuously coated fiber yarns, two additional runs were made. Process conditions, strengths and TiC coat characteristics are given in Table II.

The only difference between the coating conditions in the two runs was the $TiCl_4$ flow rate. In run No. 10 it was 0.15 ℓ(STP)/min and in run No. 11 it was 0.05 ℓ(STP)/min. Run No. 10 was made in one continuous length of 150 metres, while run No. 11 was 285 metres long, made in four segments of either 60 or 75 metres each. Samples were taken at the beginning and end of each segment for evaluation.

For run No. 10, the single-ply strength varied from 23.19 N at the beginning of the 150 metre length to 15.58 N at its end. Microscopically, the beginning and end samples looked very much alike. SEM showed the coats to be generally smooth and uniform, with occasional nodules adhering to the surfaces. Typical photomicrographs are shown in Fig. 7. Careful examination of many cross-sectional areas, however, such as those shown in Fig. 7, revealed a significantly greater number of welds between fibers at the end than at the beginning of the run. This undoubtedly is the reason for the lower strength at the end of the 150 metre length.

10

TABLE II

PROCESS CONDITIONS[a] AND RESULTS FOR TiC-COATED THORNEL 50 YARN
CONTINUOUSLY COATED IN LENGTHS UP TO 150 METRES

| Run No | Length, m | Sample Position | Tensile Breaking Load[b], N | | | Thickness, μm | | | TiC Coat Characteristics |
			mean	std dev	CV[c]	mean	std dev	CV	Microscopic Appearance (SEM)
10	150	beginning	23.19	1.39	0.06	0.10	0.03	0.35	smooth, few nodules, v few welds
		end	15.58	1.23	0.08	0.10	0.04	0.34	smooth, few nodules, welds
11A	75	beginning	23.70	1.72	0.07	0.09	0.02	0.18	smooth, few nodules, v few welds, few spalls
		end	22.79	1.07	0.05	0.10	0.02	0.23	smooth, few nodules, v few welds, few spalls
11B	60	beginning	23.96	2.59	0.11	0.10	0.02	0.21	smooth, few nodules, v few welds
		end	23.09	2.29	0.10	0.09	0.02	0.21	smooth, few nodules, v few welds
11C	75	beginning	25.14	1.66	0.07	0.09	0.02	0.22	smooth, few nodules, v few welds, few spalls
		end	23.95	2.37	0.10	0.09	0.02	0.23	smooth, few nodules, v few welds, few spalls
11D	75	beginning	23.63	1.21	0.05	0.10	0.02	0.19	smooth, few nodules, v few welds
		end	24.93	1.22	0.05	0.10	0.02	0.23	smooth, few nodules, v few welds, few spalls
Control[d]	---	---	22.38	2.14	0.10	0	---	---	---

[a]Coating Gas Flow Rates: 14ℓ(STP)/min H_2, 12ℓ(STP)/min He, 0.15ℓ(STP)/min $TiCl_4$ (Run No. 10), 0.05ℓ(STP)/min $TiCl_4$ (Run No. 11A through 11E). An additional 2ℓ(STP)/min He at top (fiber exit) gas seal. Deposition Conditions: 15 seconds at 1450 K (yarn feed rate = 1.0 m/sec).

[b]Measured on one ply of two-ply yarn.

[c]Coefficient of variation (std. dev. ÷ mean).

[d]Uncoated, as-received, PVA-sized Thornel 50.
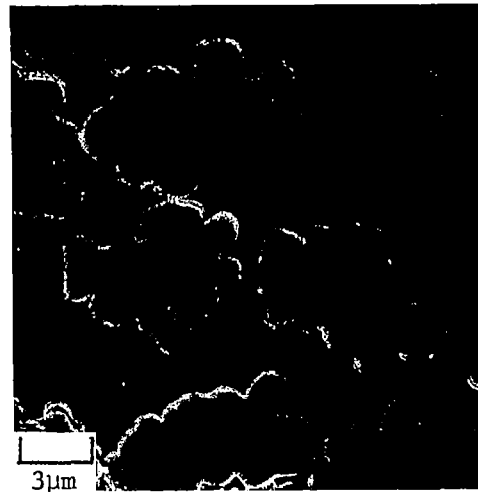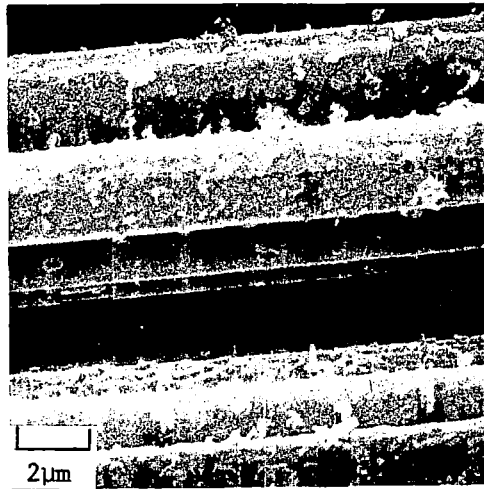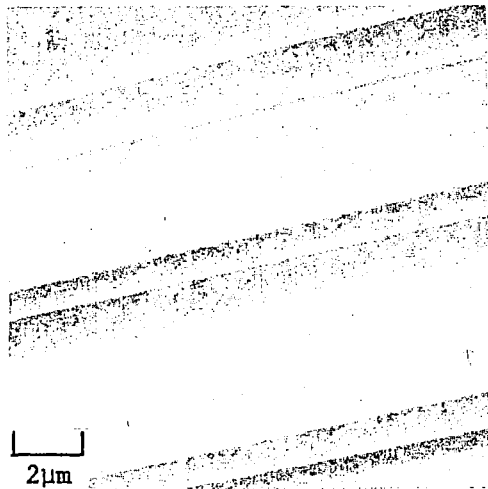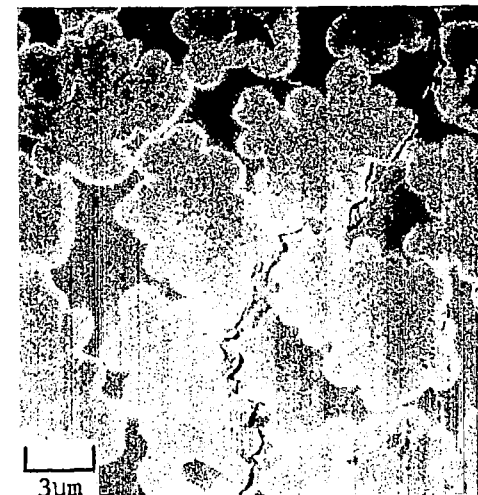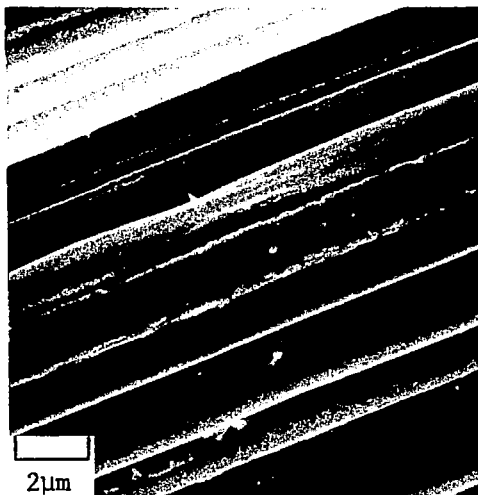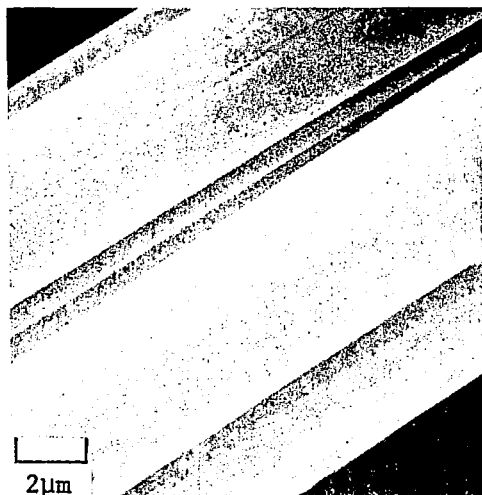
END OF COATING RUN

Fig. 7. SEM photomicrographs of samples from beginning and end of TiC coating run No. 10. Left: smooth TiC coat, typical of most fibers in run. Middle: nodules and occlusions (not typical). Right: cross sections showing uniformity of coats.

SEM examination of the samples from run No. 11 showed the coats to be smooth and uniform with few nodules. There appeared to be very few welds between fibers, but a few spalls were observed in several of the samples. Photomicrographs showing the typical smooth, uniform coat seen on most of these fibers, and an example of the infrequently occurring spalls are shown in Fig. 8. The spalls seemed not to affect the strength, which appeared to be fairly constant for the four segments, regardless of the presence of spalls.

Compaction

Eleven successful compaction runs were made to consolidate Al-infiltrated Thornel 50 graphite fibers into small bars for flexure testing. Of these, eight were made with infiltrated TiC-coated fibers prepared at LASL, and three were made from commercially-infiltrated Thornel 50 produced by Fiber Materials, Inc. (FMI). The fibers in the commercial product were chemically treated by a proprietary FMI process to promote wetting. Whatever the chemical treatment used, it apparently did not leave a permanent coat on the fibers, since none could be detected microscopically. The compacted bars were tested in four-point loading and their flexure properties are listed in Table III. The testing apparatus and the calculation of the properties are discussed in APPENDIX D.

Four different lots of TiC-coated fibers were used (Table III)—two which were produced by the batch coating process (lots 2-21-75 and 3-17-75), and two by the continuous coating process (lots 4F and 4H). In these four lots the TiC coat thicknesses vary from 0.03 to 0.32 μm, and the fiber strengths from about 0.6 to 2.1 GPa.

To produce the infiltrated starting material to be used in the compaction runs, 48 two-ply strands of the TiC-coated Thornel 50, containing 1440 fibers per strand, were placed into a 6.35-mm-diam hole in a graphite infiltration mold and pressure-infiltrated at 0.69 MPa with a LASL-produced Al-13 wt% Si alloy (Lot XI-432). The chemical analysis of this alloy is as follows: 12.7% Si, 0.4% Fe, 0.06% Cu, 0.04% Mg, 0.03% Mn, <0.01% Zn, remainder Al. The infiltration method and apparatus were described previously.[3] In each infiltrated sample there were 69,120 fibers, each with a nominal diameter of 6.5 μm. The ratio of the total cross-sectional area of these fibers, to the cross-sectional area of the hole which contains them in the infiltration mold, is approximately 0.007. Therefore, in an infiltrated sample there is a large excess of matrix alloy. Within the infiltrated samples the fibers tended to be grouped in a small region of the total cross sectional area. In general, most of this excess was squeezed out during the compaction operation. The degree of infiltration of three of these materials is shown in the photomicrographs of Fig. 9, together with the microstructure of the commercially infiltrated material. Here it is seen that lot 4F fibers, which had the thickest TiC coat (0.32 μm), were the best infiltrated of the TiC coated materials. Lot 3-17-75 was next best, while lot 4H was the least well infiltrated of those shown in the figure. The lot 2-21-75 fibers (not shown) had the thinnest TiC coat and underwent almost no infiltration. Although the data are few, it appears that there is a trend toward greater degree of infiltration with greater coat thickness. This is to be expected, because with the deposition of greater amounts of TiC the likelihood of uncoated fibers within the yarn should be reduced significantly. Therefore, yarns with greater average fiber thicknesses should be capable of more thorough wetting and undergo greater infiltration.

13
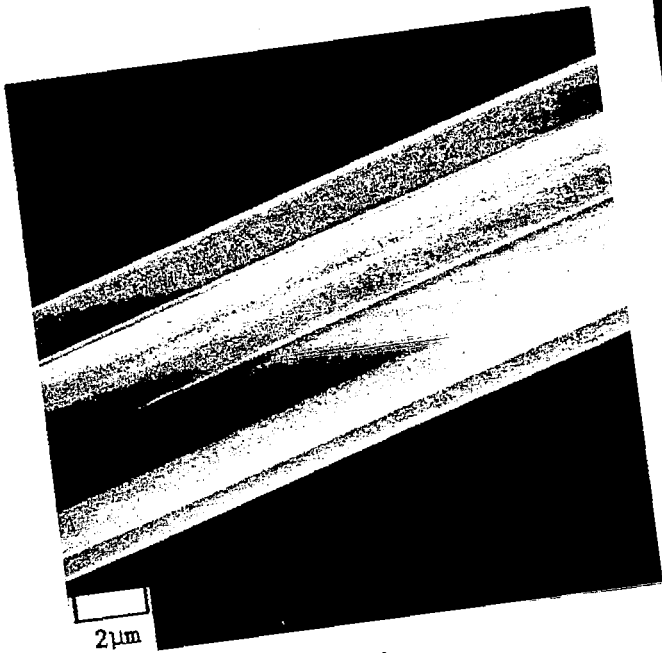
(a)
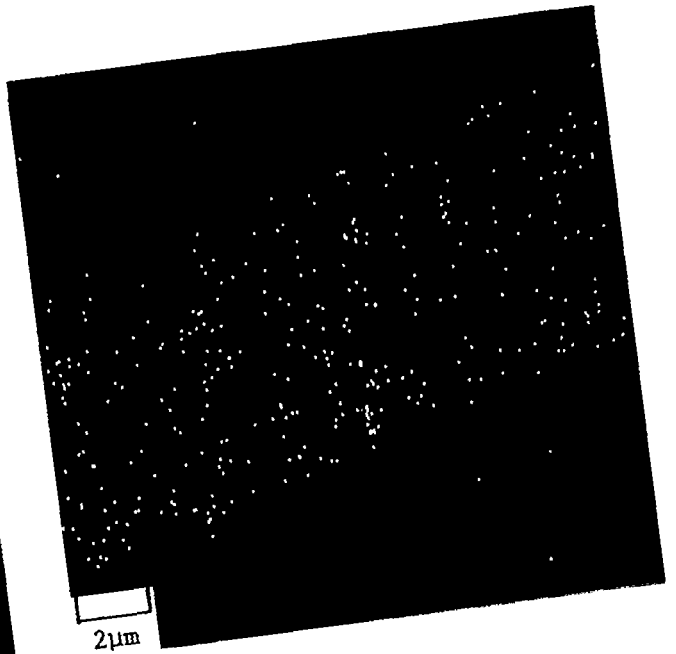
(b)
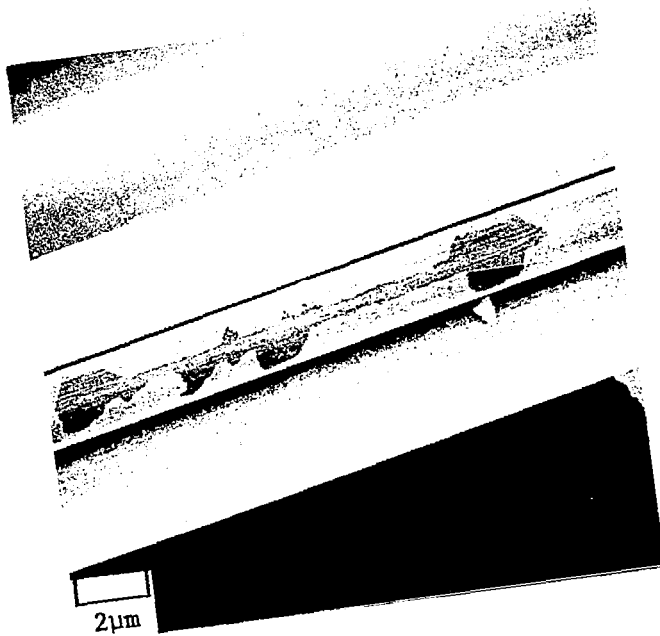
(c)

Fig. 8. SEM photomicrographs of fiber samples from TiC coating run No. 11. (a) Smooth, uniform TiC coat, typical of most fibers in run. (b) Ti x-ray scan of (a). (c) Area showing spall (not typical).

TABLE III

FLEXURE PROPERTIES OF COMPACTED THORNEL 50 YARN
INFILTRATED WITH Al-13% Si ALLOY

| Composite | Fiber Yarn | | | Composite Properties | | | | | | | | Alloy |
Sample	Lot	τ, μm	σ_f, GPa	v_f, %	w, mm	t, mm	P, N	δ, mm	σ, GPa	%ROM	ε, %	σ_a, GPa
C-3[a]	---	---	2.172	64.3	6.375	0.559	91.6	0.328	0.878	60.6	0.46	0.148
C-7[a]	---	---	2.172	60.1	6.388	0.597	83.3	0.302	0.697	51.1	0.45	0.147
C-8[a]	---	---	2.172	60.5	6.370	0.595	100.8	0.282	0.854	62.3	0.42	0.144
C-9	3-17-75	0.09	0.867	42.5	6.424	0.838	62.6	0.099	0.264	61.4	0.21	0.106
C-10	3-17-75	0.09	0.867	42.8	6.477	0.826	72.8	0.122	0.314	71.5	0.26	0.119
C-11	4F	0.32	0.556	38.0	6.502	0.927	75.0	0.338	0.256	79.7	0.79	0.178
C-12	4F	0.32	0.556	35.7	6.477	0.991	95.1	0.391	0.285	88.9	0.98	0.191
C-13	4H	0.18	2.093	29.0	6.502	1.219	98.2	0.259	0.194	26.5	0.79	0.178
C-14	4H	0.18	2.093	33.8	6.477	1.041	69.7	0.264	0.188	22.3	0.70	0.171
C-19	2-21-75	0.03	1.431	44.4	6.452	0.800	61.3	0.467	0.283	38.2	0.95	0.189
C-22	2-21-75	0.03	1.431	45.1	6.452	0.787	49.7	0.437	0.237	31.7	0.88	0.184

τ = TiC coat thickness on individual fibers

σ_f = strength of individual fibers

v_f = volume percentage fibers in compacted composite

w = width of sample

t = thickness of sample

P = load at fracture

[a]Made from samples infiltrated by FMI

δ = deflection at fracture

σ = stress at fracture

%ROM = percentage of rule-of-mixtures
strength (σ/σ_c, see APPENDIX D)

ε = strain at fracture

σ_a = stress in Al-13% Si alloy at
strain ε
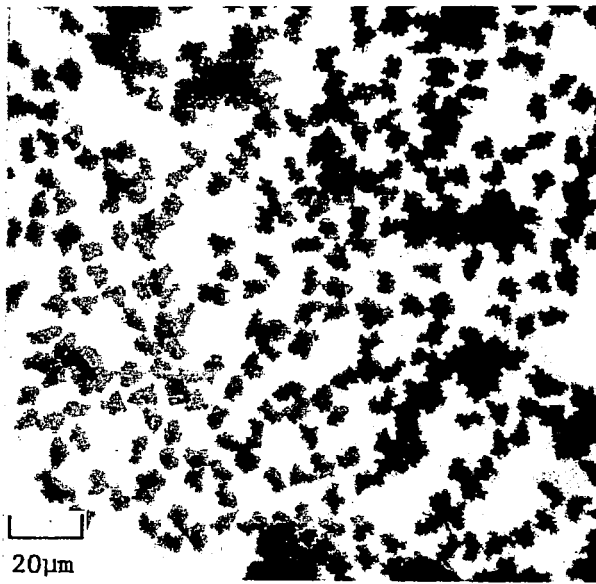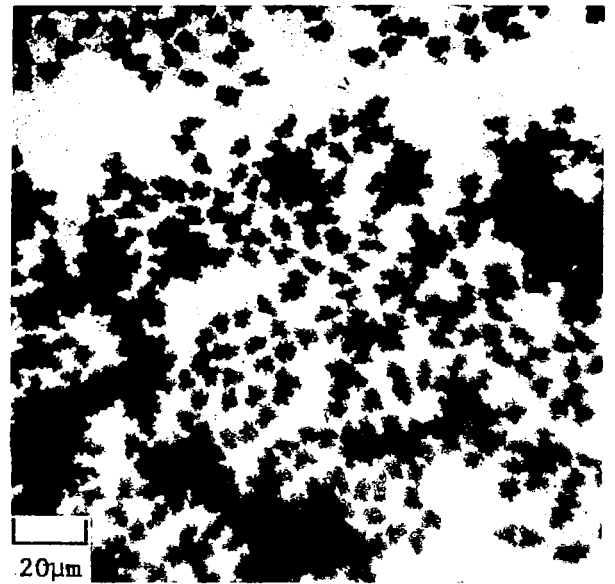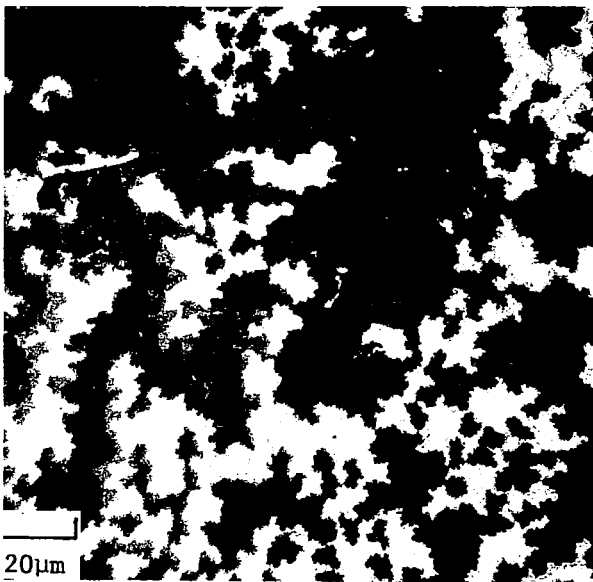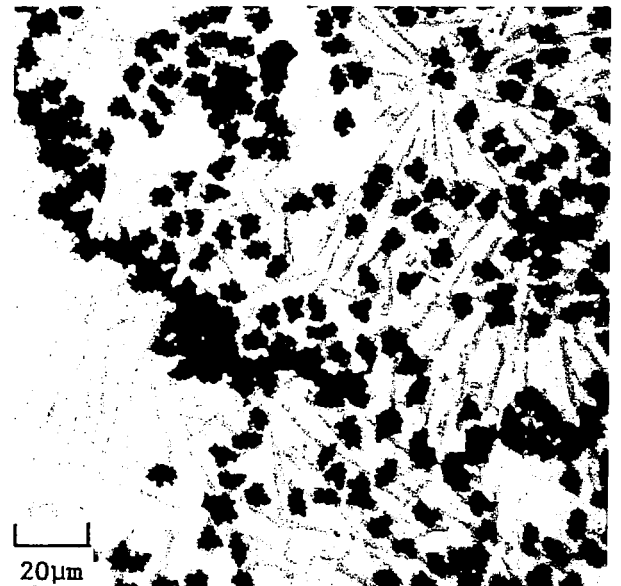
Fig. 9. Aluminum-infiltrated Thornel 50 fibers used in compaction experiments.
(a) TiC-coated fibers, lot 4F, compacted in samples C-11 and 12.
(b) TiC-coated fibers, lot 3-17-75, compacted in samples C-9 and 10.
(c) TiC-coated fibers, lot 4H, compacted in samples C-13 and 14.
(d) Uncoated (commercially infiltrated) fibers, compacted in samples
C-3, 7 and 8.

After infiltration the resulting composite rods were cleaned by light sanding of their surfaces, placed into a rectangular graphite compacting mold (Fig. 10) approximately 6.35 mm wide and 38 mm long, and vacuum hot-pressed at 1.35 MPa and a maximum temperature of 930 K. The commercially-infiltrated starting material was originally in the form of a composite wire containing eight two-ply strands of uncoated Thornel 50 in an Al-13% Si matrix. Six lengths of this wire, 38 mm long, also containing 69,120 fibers, were similarly vacuum hot-pressed.

A schematic of the hot pressing assembly and a typical hot pressing cycle are shown in Figs. 11 and 12, respectively. The graphite compacting mold containing the infiltrated fibers is placed within the vacuum vessel and evacuated to a pressure of about 0.1 mPa ($\sim 10^{-5}$ mm Hg). No heat or external load is applied at this point. The furnace for heating the hot pressing assembly is located directly below the vessel on the hydraulic lift. The general arrangement of this system is shown in Fig. 13. When the furnace temperature reaches 1223 K the furnace is raised to a position surrounding the vacuum vessel, and the graphite mold containing the infiltrated fiber samples then rapidly heats up (Fig. 12). At a sample temperature of 903 K, which is ~ 50 K above the alloy solidus, the furnace is lowered away from the vessel and a dead-weight load, corresponding to 1.38 MPa, is applied to the compacting mold. The sample continues to heat up to about 930 K before cooling begins. When it finally cools to about 770 K the load is removed. Typically, the sample remains at temperatures above the solidus for approximately nine minutes. Throughout the compaction experiment, the vacuum in the vessel will vary with temperature (due to outgassing), as shown in Fig. 12. The final size of the flexure bars was approximately 38 mm long, 6.4 mm wide and varied in thickness from about 0.6 mm to 1.2 mm (Table III).

In Table III the strengths of the compacted composites are given both as the stress at fracture, σ, and as the percentage of the rule-of-mixtures strength, % ROM ($= \frac{\sigma}{\sigma_c} \times 100$). The rule-of-mixtures strength is defined as the volume-fraction weighted average strength given by

$$\sigma_c = v_f \sigma_f + v_a \sigma_a ,$$

where v_f and v_a are the volume fractions of the fibers and the aluminum alloy matrix, respectively, in the composite, σ_f is the strength of the individual fibers, and σ_a is the stress in the alloy corresponding to the strain (ε) at which fracture occurred in the composite. Neither σ or % ROM are completely suitable parameters for comparing the strengths. To compare the σ values directly makes the composites with the coated fibers look poor, relative to the compacted commercial material (C-3, 7 and 8). For the commercial material the average σ is about 0.8 GPa, whereas for the composites containing the coated fibers the σ values are less than half as great, varying from about 0.19 to 0.31 GPa. The differences between the σ values of the commercial and the coated fiber composite materials is primarily due to two factors: the TiC-coated fibers (1) have lower strengths (σ_f) than does the uncoated fiber and
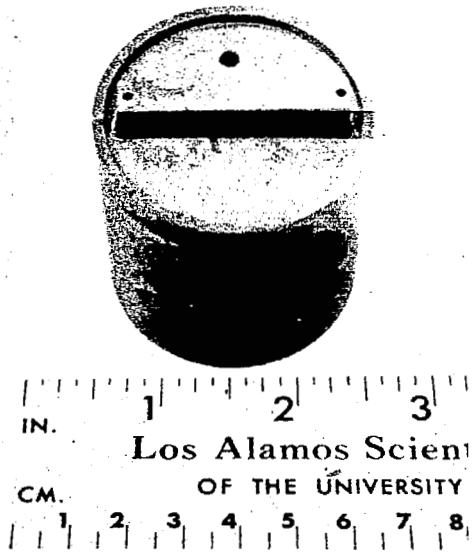
Fig. 10.   Graphite compacting
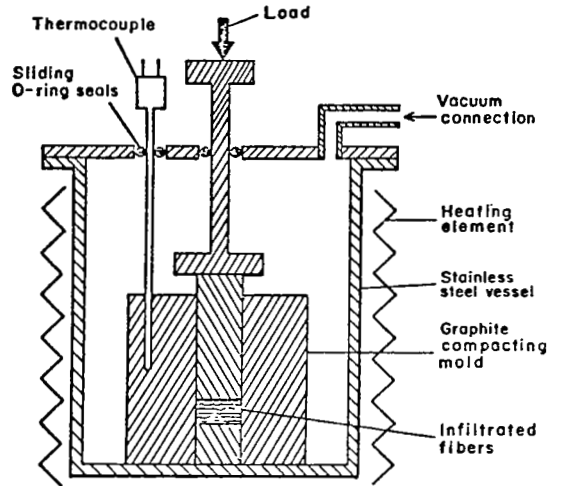   mold.

Fig. 11.   Schematic of vacuum hot-
           pressing system.

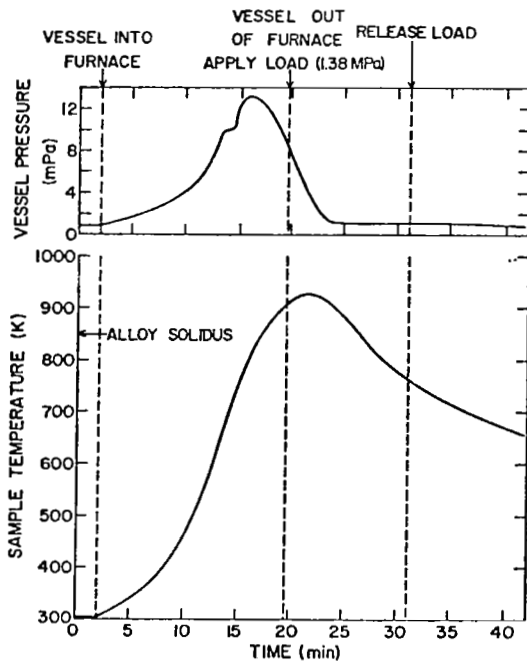
Fig. 12.   Typical hot-pressing
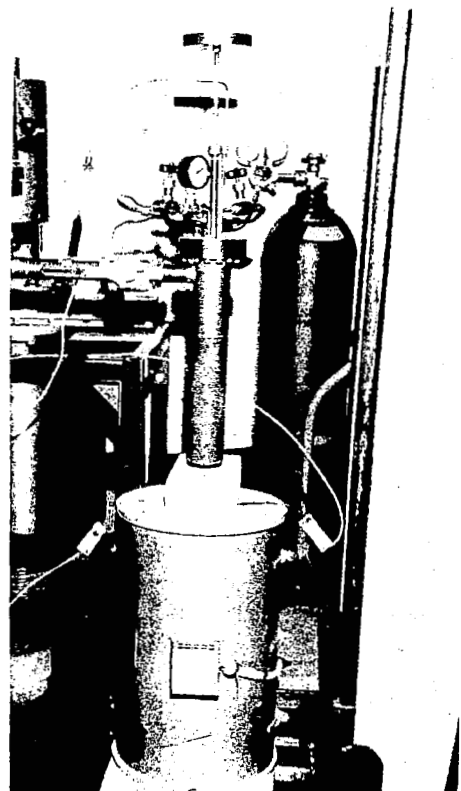   cycle.

Fig. 13.   Vacuum hot-pressing
           apparatus.

18

(2) have much lower concentrations (v_f) in the composite.[*] Both of these factors contribute toward the lower strength (σ) of the coated-fiber composites, compared with the commercial. However, by normalizing the composite strengths by use of above formula for σ_c, and computing the % ROM, some of the coated fiber composites appear significantly better than the commercial material. The percentage ROM ranged from 22% to nearly 90% for the coated fiber composites, while for the commercial material it ranged from 51% to 62%. Although the % ROM may be a measure of the effectiveness of composite manufacture, the actual strength (σ) is the important value from the practical, design standpoint. Therefore, the coated-fiber composite materials in Table III would not be considered as serious competition to the commercial material for strength applications.

The low strengths (σ) of the composites made with coated fibers, compared with those made with the commercial material, are due not only to the lower strengths and volume fractions of the coated fibers, but also to their ability to be wetted by the aluminum alloy. The wettability tends to increase with coat thickness and, of course, the better the wetting the greater the strength of the composite. The wettability and the strength of the fibers seem to be competing factors in the strength of these composites. That is, as coat thickness increases, the strength of the composite will decrease due to the decrease in strength of the coated fibers (Figs. 5 and 6), but will increase due to their better wettability. For such a composite system there undoubtedly is an optimum TiC coat thickness which should balance these two factors to give the maximum strength. Unfortunately, time did not permit the desired follow-up in this area.

A comparison of the % ROM data of Table I with the photomicrographs of Fig. 9 illustrates the relationship between the strength of the composites and the degree of infiltration of the fibers. Note, for example, that the best infiltrated of the TiC-coated fibers (lot 4F, Fig. 9a) yielded the highest ROM strength (C-11 and 12, Table III), and the most poorly infiltrated fibers (lot 4H, Fig. 9c) yielded the lowest strength (C-13 and 14). Compaction of these infiltrated fibers did little to improve the distribution of fibers in the alloy matrix or the apparent infiltration of the fibers. Cross-sections of the compacted samples were examined microscopically and showed little, if any, change in the degree of infiltration of these materials when compared with Fig. 9. This observation confirms the great importance of starting with well-infiltrated material in the manufacture of graphite-aluminum composites.

It is not necessarily true that only fibers with thick TiC coats wet well with aluminum alloys. As was pointed out above, the trend of increasing wettability with increasing coat thickness was probably due to the greater amounts of deposited TiC reducing the likelihood of uncoated regions on the fiber surfaces. Therefore, wettability is actually related not to coat

---

[*] Another source of uncertainty is in the strength of the fibers used in the commercial material. The same value for the manufacturers strength, σ_o (APPENDIX D), was used throughout the calculations. In fact, it has been the experience here that fiber strength may vary significantly from point to point in a spool of yarn as well as from spool to spool.

thickness but to the efficiency of coating—i.e., fiber coverage. Yarns with thin, uniform coats on the individual fibers, then, should be just as easily wetted and infiltrated as are those with thick coats, provided the fibers have a thorough coverage. Again, because of time limitations, some of the more promising coated fibers produced in the latter stages of this study, particularly in Series No. 9, were not evaluated for their usefulness in graphite-aluminum composites. These fibers, typically, had smooth, thin coats and were of particularly high strength (Table I).

During the flexure tests, the samples typically gave sharp breaks in the stress-strain curve at the point of failure. However, none of the samples broke completely into two pieces. (A typical stress-strain curve and a failed sample are shown in APPENDIX D.) To evaluate fracture character, four of the failed specimens were completely broken by hand into two pieces. The fracture surfaces of these are shown in the SEM photomicrographs of Fig. 14. It is clear that there is a significant difference between the fracture character of sample C-8 which was made from commercially infiltrated, uncoated Thornel 50 fibers, and the other three (C-9, C-12 and C-14), whose fibers had been coated with TiC. Although it was at least as well infiltrated as any of the others, C-8 had a more fibrous appearing fracture; bundles of many fibers, as well as individual fibers, pulled out of the sample. In sample C-12, however, fracture was uniform over large areas, with much less pullout. Sample C-9 was similar to C-12, except that there were some areas that were nearly all matrix material, containing very few fibers. This is seen in Fig. 14 as stringers of a light phase material. C-14, on the other hand, had very large areas—some covering the entire thickness of the sample—that were essentially all matrix material (Fig. 14). Its fracture in the composite areas was similar to that of C-9 and C-12.

Pullout was observed in all of the samples, but to a much greater extent in the commercially-infiltrated material (C-8). A typical example of pullout is shown in Fig. 15. The smaller amount of pullout observed for the TiC-coated fibers, relative to that for the uncoated fibers, indicates that better bonding with the matrix alloy is achieved with the TiC-coated fibers.

In all of the samples there was some fragmentation of both fibers and matrix material at the fracture surface. This was most pronounced in the commercially-infiltrated material (C-8). An example of fragmentation is shown in Fig. 16.

Diffusion Barrier Experiments

To evaluate the effectiveness of thin TiC coats as diffusion barriers to inhibit reaction between carbon and aluminum, samples of TiC-coated, Al-infiltrated Thornel 50 fibers were heated for prolonged periods at elevated temperatures. In previous experiments,[3] heat-treatment temperatures both above and below the aluminum alloy solidus were used. At temperatures up to within 50 K of the alloy solidus no reaction occurred in samples containing either coated or uncoated fibers. Above the solidus, reaction occurred for both materials, but less extensively for the coated fibers.
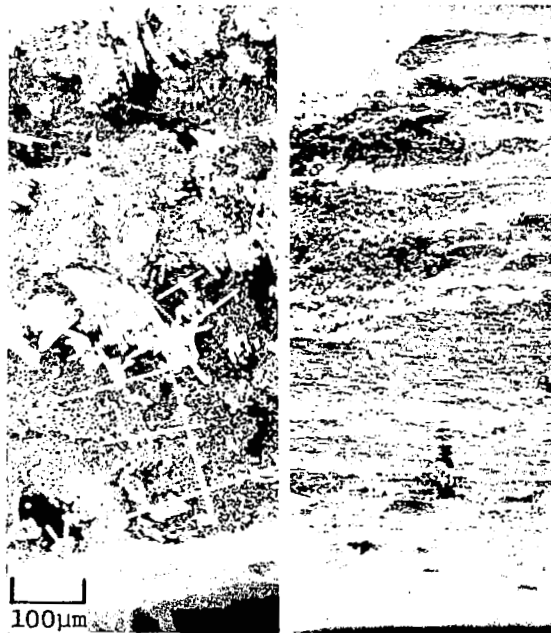
C-8
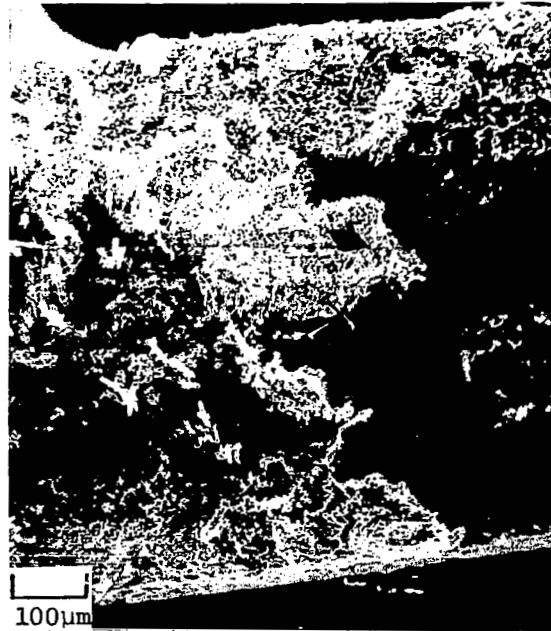
C-12
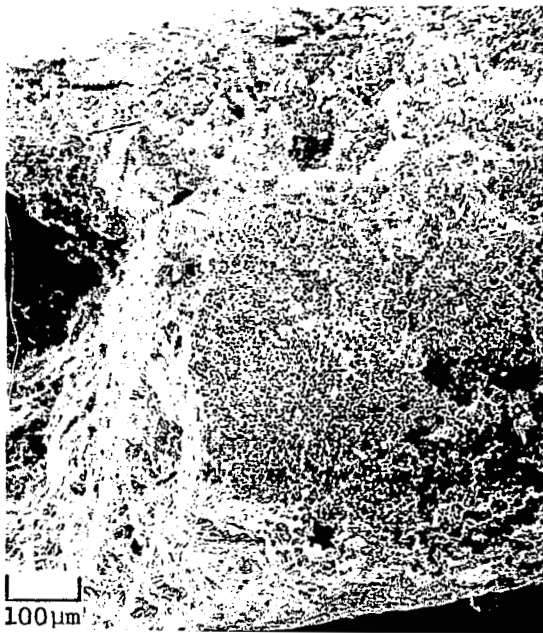
C-9

C-14

Fig. 14. SEM photomicrographs of fracture surfaces of compacted aluminum-graphite fiber composites after flexure testing. For sample C-14 two areas are shown illustrating extreme inhomogeneity: typical composite (left) and aluminum-rich area (right).
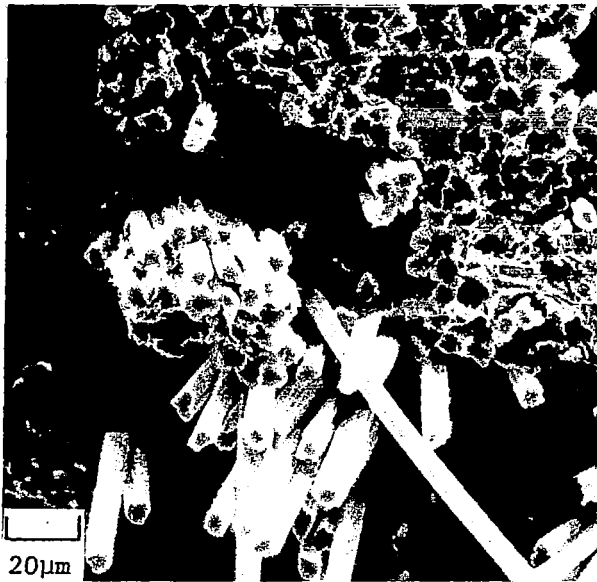
Fig. 15. SEM photomicrograph illustrating pullout of individual fibers and bundles of fibers during flexure testing (Sample C-9).

Fig. 16. SEM photomicrograph illustrating fragmentation during flexure testing (Sample C-8).

In the present experiment, heat-treatment temperatures up to within a few degrees of the solidus were used. Three samples of TiC-coated Thornel 50 yarn, infiltrated with the Al-13% Si alloy, and three of the commercially-infiltrated, uncoated Thornel 50 were heated for 100 h in flowing, purified argon. The extent of reaction was judged by the formation of a dark needle-like phase which was believed to be Al_4C_3. Temperatures and microscopic appearances of the heat-treated samples are given in Table IV. As seen, up to within 15-20 K of the solidus only a trace of reaction, at most, was observed for either coated or uncoated fibers. To within 3-8 K of the solidus temperature, however, definite reaction occurred in both materials, but much less extensively for the TiC-coated fibers.

CONCLUSIONS

1. A continuous CVD coater was constructed and was used successfully to produce thin, uniform, adherent coats of TiC on the individual fibers of graphite yarns in continuous lengths of up to 150 metres.

2. Vacuum hot-pressing was used to produce graphite-aluminum composites from TiC-coated graphite fibers infiltrated with an aluminum alloy. The strength of these composites was less than half that of a control material similarly produced from commercially infiltrated fibers. This discrepancy was due mainly to the lower strengths of the coated fibers and to their lower volume

TABLE IV

DIFFUSION BARRIER EXPERIMENTS

Sample No.	Diffusion Couple (Alloy/Substrate)	Alloy Solidus K	HTT[a] K	Microscopic Appearance
AD-14A-1	Al-13% Si/TiC-coated Thornel 50	855[b]	847	slight reaction
AD-14A-2	Al-13% Si/Thornel 50 (FMI)[d]	850[c]	847	reaction
AD-14B-1	Al-13% Si/TiC-coated Thornel 50	855[b]	835	trace reaction
AD-14B-2	Al-13% Si/Thornel 50 (FMI)[d]	850[c]	835	trace reaction
AD-14C-1	Al-13% Si/TiC-coated Thornel 50	855[b]	825	trace reaction
AD-14C-2	Al-13% Si/Thornel 50 (FMI)[d]	850[c]	825	trace reaction

[a]Heat treatment temperature. Held for 100 h in flowing, purified argon.

[b]Determined by thermal arrest, on heating, during infiltration.

[c]Al-Si eutectic temp. (Metals Handbook, 8th edition, Vol. 8, p. 263, American Society for Metals.)

[d]Uncoated Thornel 50 fiber yarns infiltrated with Al-13% Si by Fiber Materials, Inc. (FMI).

fractions in the composites. However, by normalization using the rule-of-mixtures, values as high as 90% of the rule-of-mixtures strength were achieved for composites made with the TiC-coated fibers.

3. Thin coats of CVD-deposited TiC on graphite fibers inhibit reaction between the graphite fibers and aluminum at elevated temperatures.

APPENDIX A

CONTINUOUS COATING SYSTEM AND PROCEDURES

Coating System

Coating operations are performed in an assembly basically consisting of a double-wall, water-cooled, stainless steel shell and an inductively heated inner graphite susceptor through which are passed the fibers to be coated. A photograph and schematic of the system are shown in Figs. A1 and A2, respectively. The susceptor is 102 mm outside diameter, 76 mm inside diameter and 690 mm long. The coating zone occupies approximately 250 mm in the center of the susceptor. Thermocouple wells are drilled to various depths in the wall of the susceptor, and temperature is measured over its length with Pt-Pt 10% Rh thermocouples which are shielded in alumina tubes.

By passing a thermocouple probe through the center of the furnace, temperature measurements were made along its axis at three different power settings. The temperature profiles within the furnace are shown in Fig. A3. These temperatures were correlated with those measured in the susceptor wall, and the values given in this report (Table I) were those corresponding to the center of the coating zone.

Each end of the susceptor is fitted with a graphite entrance tube which includes an inert gas connection and a 3 mm entrance orifice through which the fiber tow passes. The coating gases enter at the top of the furnace and exit at the bottom into an exhaust duct. The fibers are fed into the bottom and pulled through the furnace in a direction countercurrent to the flow of the coating gases. A gas seal is made at the top with helium and at the bottom with argon. Careful adjustment of the gas flows at each seal and of the pressure on the exhaust is necessary to exclude air from the furnace. The fibers are fed into the furnace from a spool of commercial graphite yarn. To remove any twist in the yarn, the spool is mounted in a fixture, shown in Fig. A4, such that it can be rotated about an axis perpendicular to the axis of the spool. This detwister is equipped with a reversible, variable speed motor. As it is pulled from the spool, the yarn passes over a graphite pulley (Fig. A4) and into the furnace. The coated fibers emerge from the top of the furnace, pass over another graphite pulley, and are wound onto a take-up spool, which is mounted on a spooler. To distribute the yarn uniformly, a spool traverse plays the fibers back and forth on the take-up spool. The spooler and traverse are shown in Fig. A5. Both are equipped with reversible, variable speed motors.

$TiCl_4$ coating gas is fed into the furnace from an evaporator, shown in Fig. A6. The $TiCl_4$ is heated to about 350 K with a standard laboratory heating tape. Helium is bubbled through the $TiCl_4$, carrying it out of the evaporator, where it combines with the other constituents of the coating gas (Fig. A2). All lines carrying these gases are heated with heater tapes. Coating gas flow rate is varied by varying the temperature of $TiCl_4$ and the flow rate of the helium carrier gas.
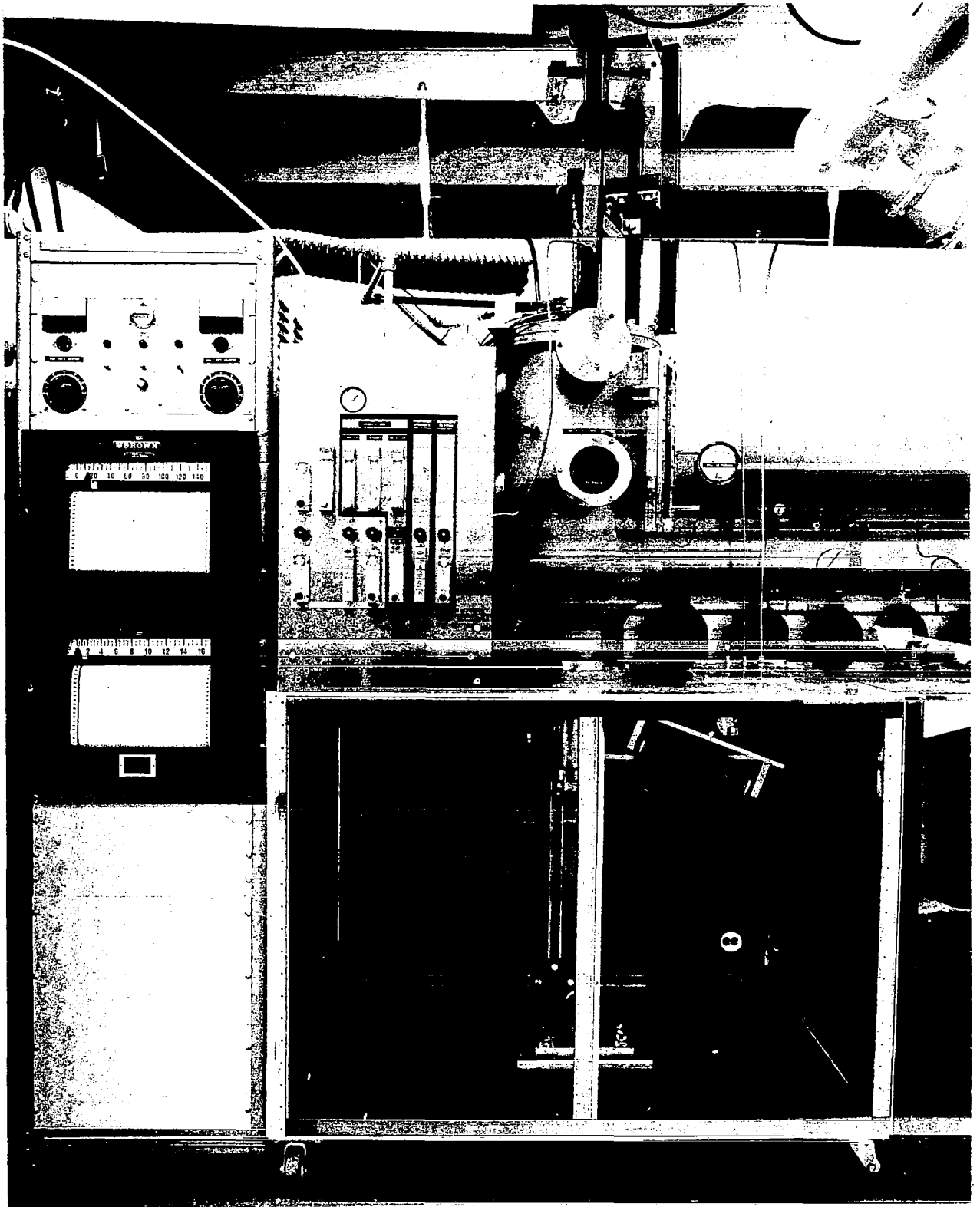
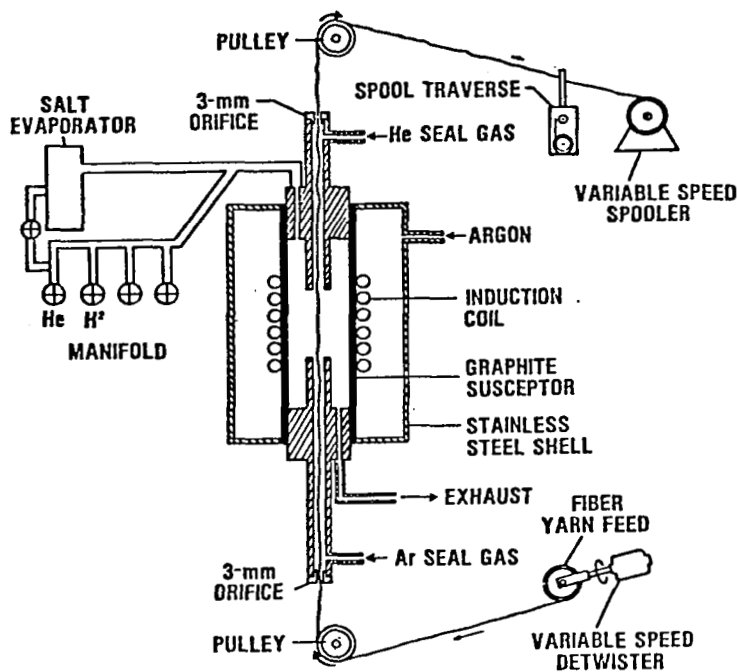Fig. A1.   Overall view of continuous coating apparatus.

Fig. A2.   Schematic of system for continuous coating
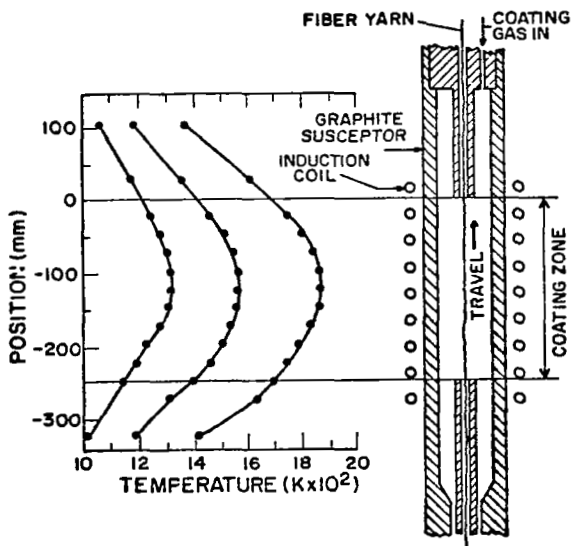of graphite fibers with TiC.

Fig. A3.   Temperature profiles in
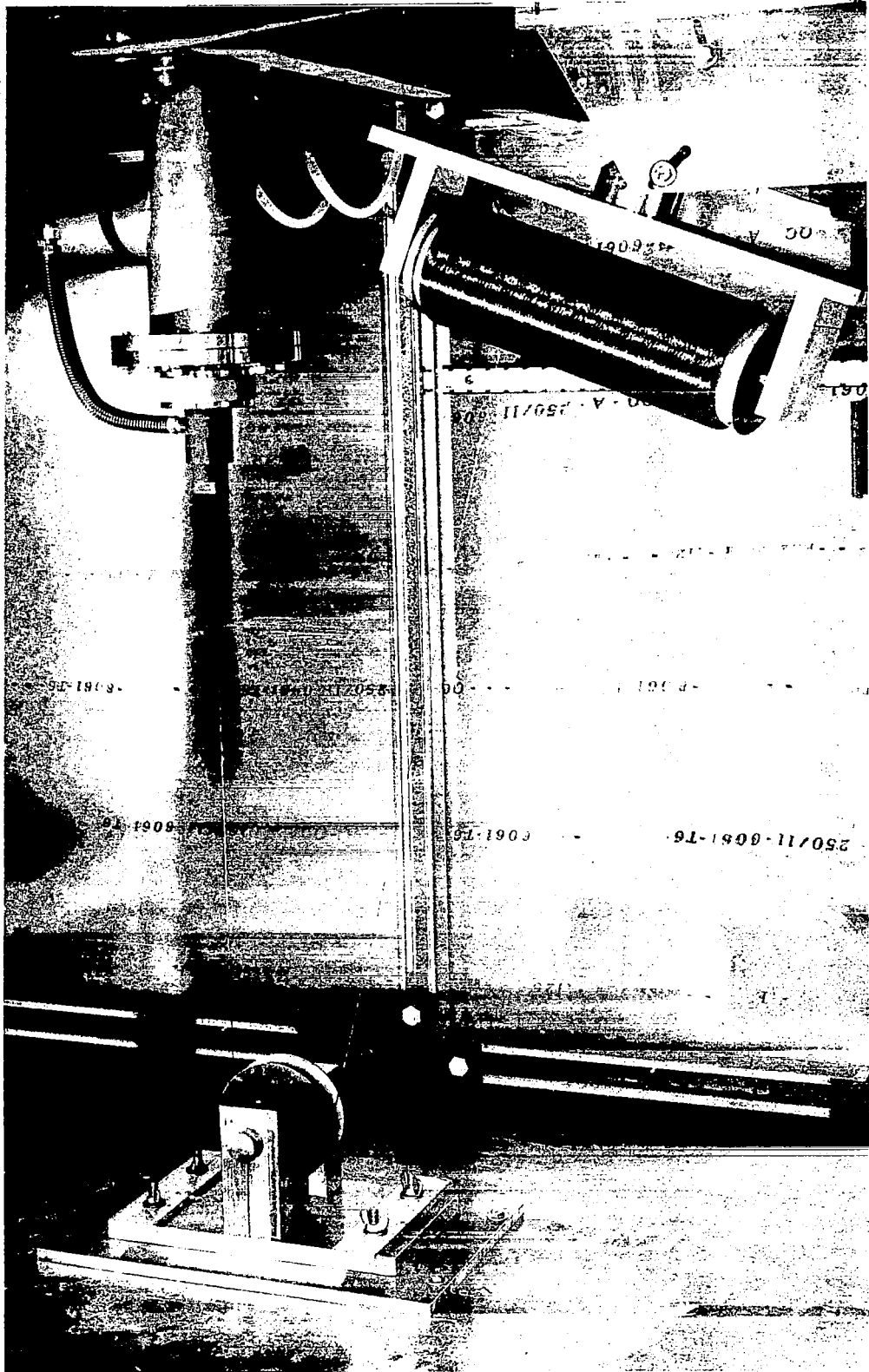coating zone at three
different power settings.
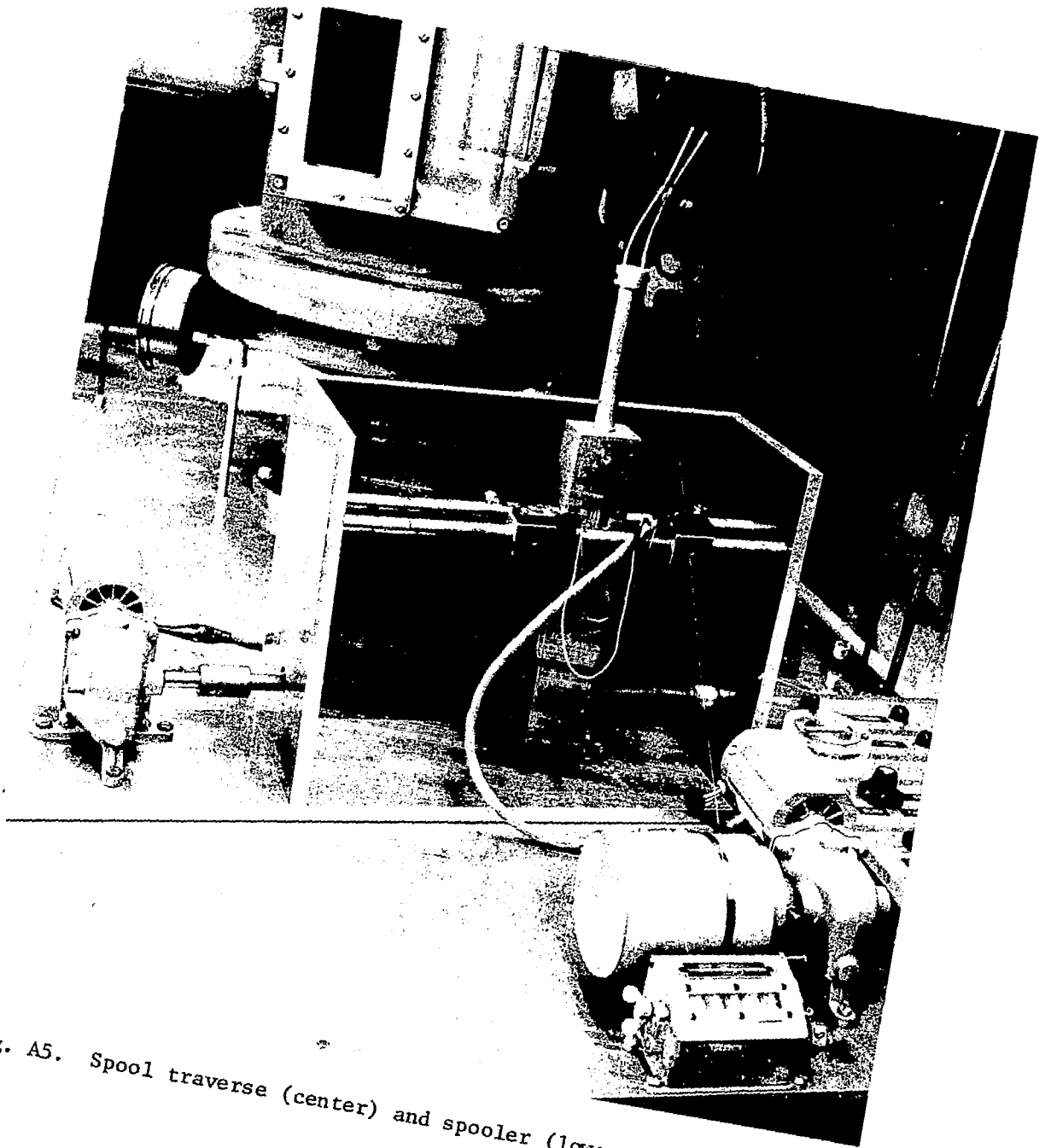
Fig. A4. Fiber feed system.

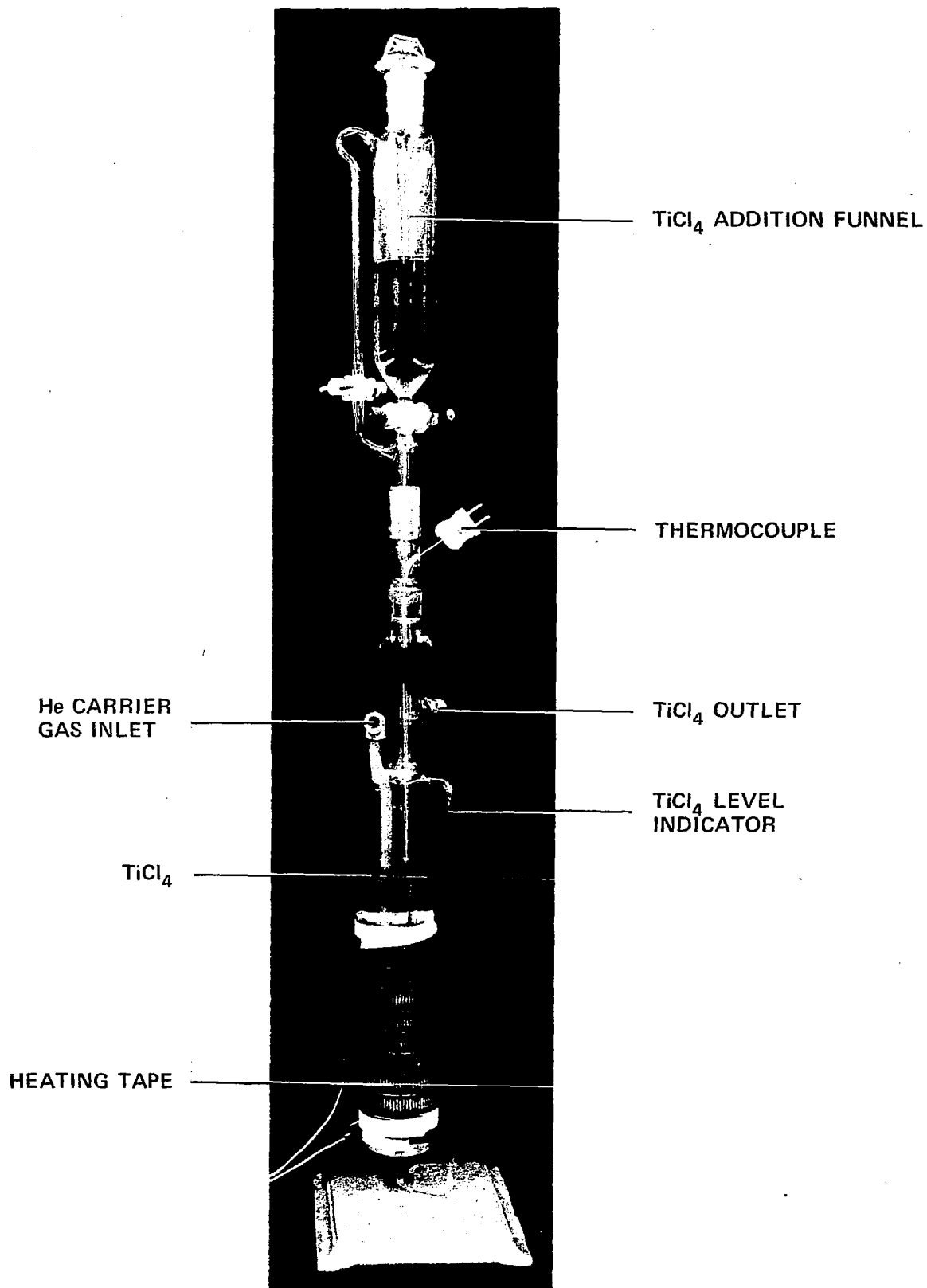Fig. A5. Spool traverse (center) and spooler (lower right).

TiCl$_4$ ADDITION FUNNEL

THERMOCOUPLE

He CARRIER
GAS INLET

TiCl$_4$ OUTLET

TiCl$_4$ LEVEL
INDICATOR

TiCl$_4$

HEATING TAPE

Fig. A6. TiCl$_4$ Evaporator.

30

Operation

Before beginning each run, the yarn to be coated is passed through the bottom pulley, threaded through the bottom entrance orifice, attached to a heavy graphite yarn (which was dropped through the furnace from the top) and pulled through the furnace. It is then passed over the top pulley and attached to the take-up spool on the spooler. The top orifice, which consists of split halves, is placed in position where the fiber exits from the furnace. Start up of the coating system consists of the following steps:

1. Spooler, spool traverse and detwister are started and adjusted to the desired speeds.

2. Seal gases are introduced and adjusted.

3. Exhaust pressure is adjusted to slightly below atmospheric ($\Delta P = -30$ to -50 Pa).

4. Manifold helium and hydrogen are introduced and adjusted.

5. Power is turned on to induction coil.

6. At the desired temperature, helium is introduced to the preheated evaporator and coating begins.

Usually, it is necessary to readjust the seal gas flows until the emerging fibers have the characteristic metallic gray color of TiC. Without this adjustment, air is admitted to the furnace and fibers are oxidized to a blue or green color.

TESTING FIBER STRENGTH

Samples of two-ply yarn are cut to about 140 mm lengths and the plys sepa-
rated. The ends of the single-ply lengths are then sandwiched between the ad-
hesive sides of two pieces of masking tape, approximately 50 mm by 50 mm in area.
These masking tape tabs are separated in the central length of the sample by ap-
proximately 23 mm. A sample is tested by clamping the tabs between parallel flat
grips, separated by 25.4 mm, in a tensile tester and pulling to failure. The ten-
sile breaking load values are reported in newtons (N).
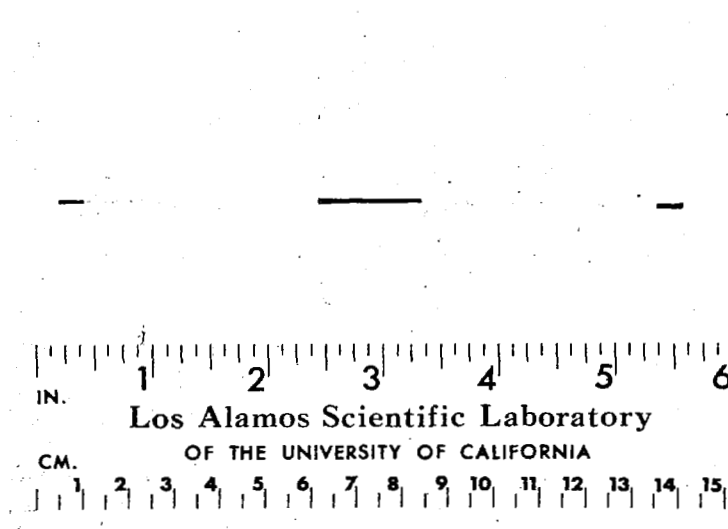
Fig. B1. Single-ply fiber yarn with masking
tape tabs, ready for tensile testing.

APPENDIX C

SURFACE MORPHOLOGIES OF TiC-COATED

THORNEL 50 FIBERS

(a)   (b)
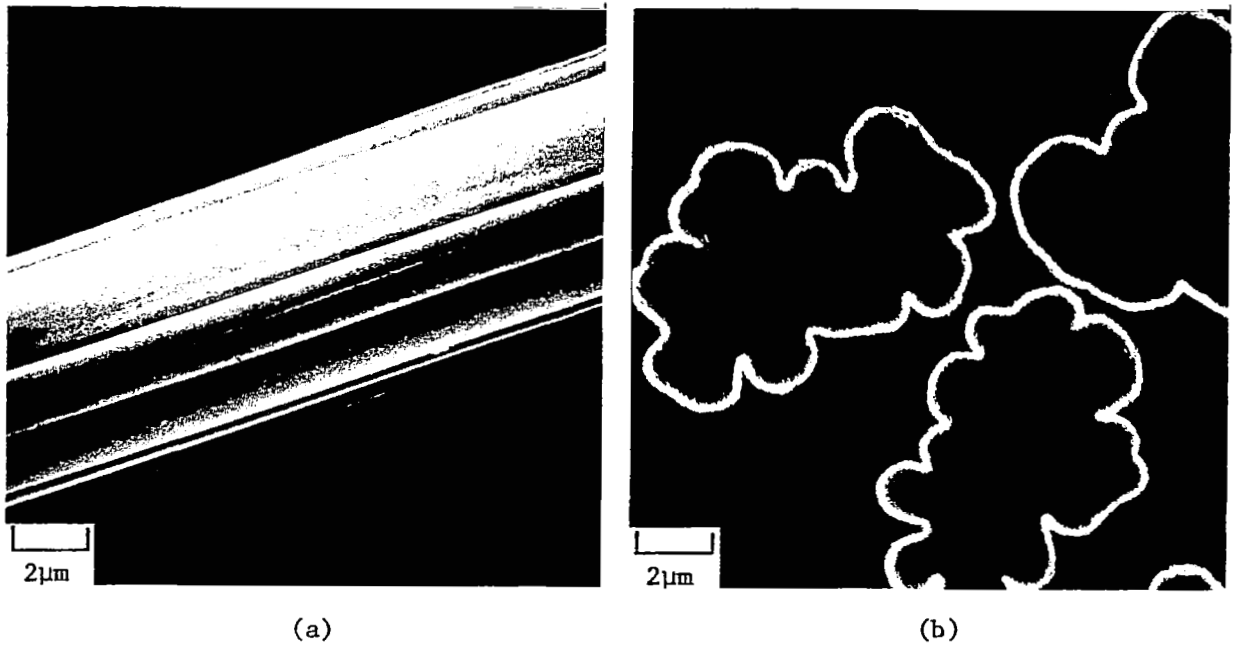
Fig. C1. Typical example of smooth, uniform, adherent TiC coat on graphite fibers.
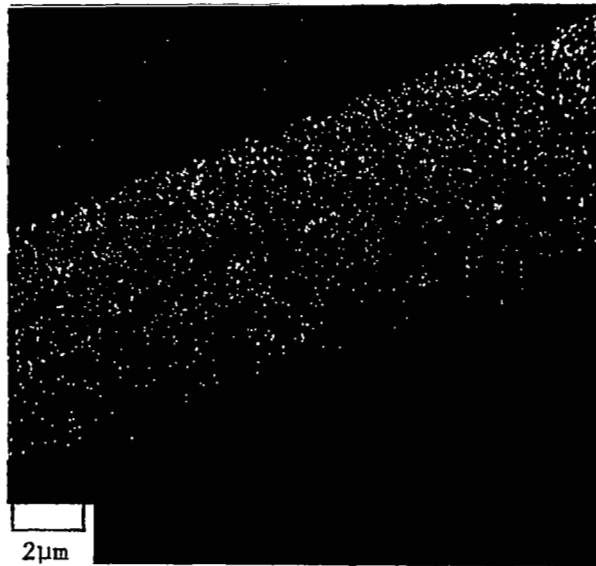   (a) Surface. (b) Polished cross section (Run 4E).

(a)   (b)
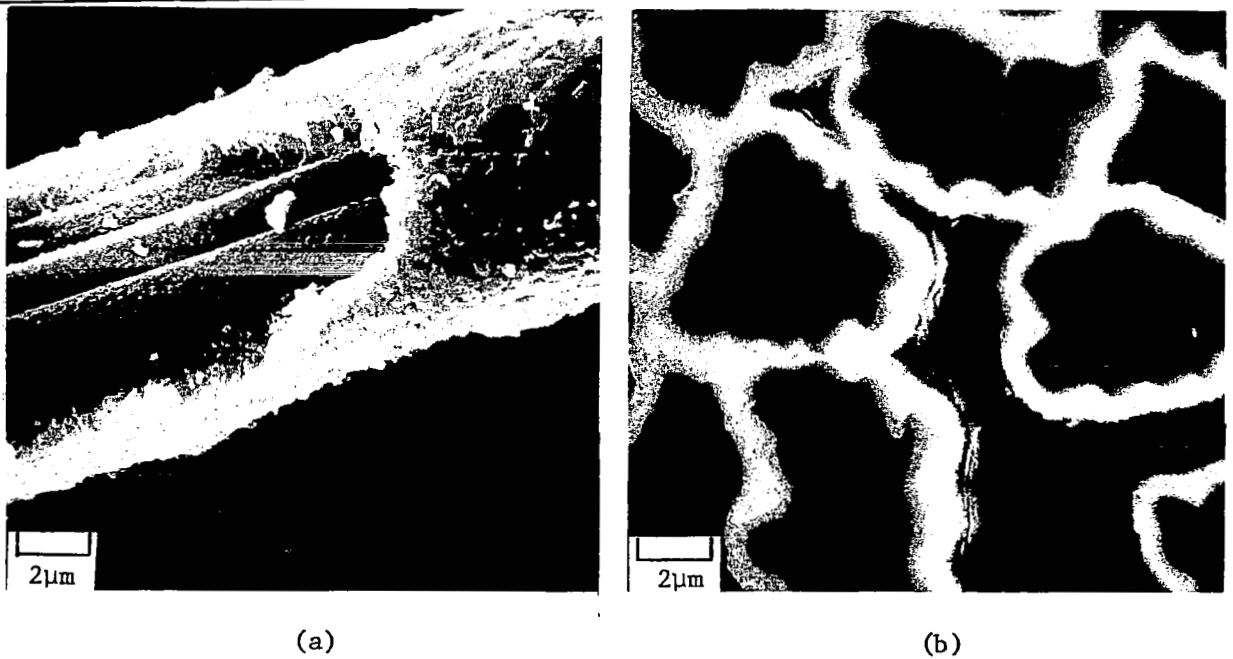
Fig. C2. Example of rough TiC coat showing typical (a) spall on fiber surface
          and (b) welding between fibers (Run 1B).
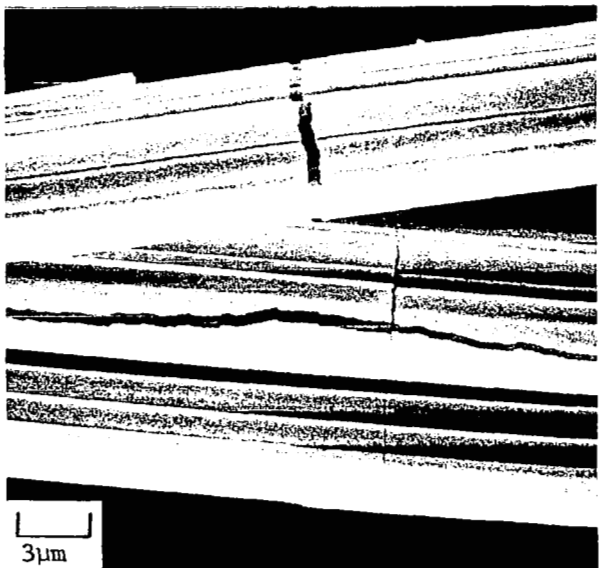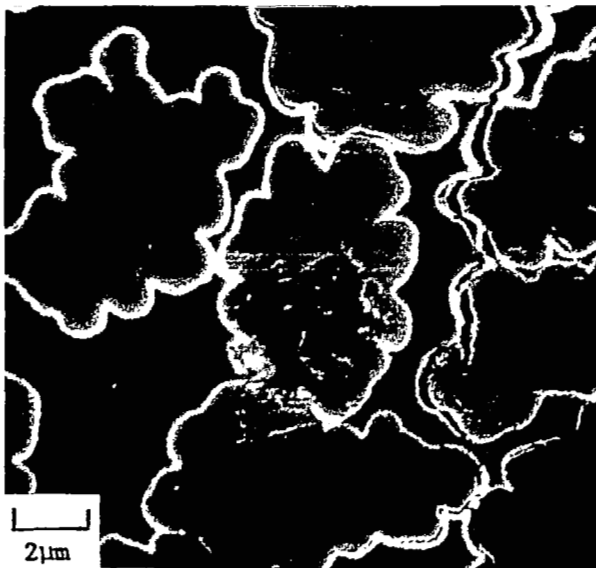
34
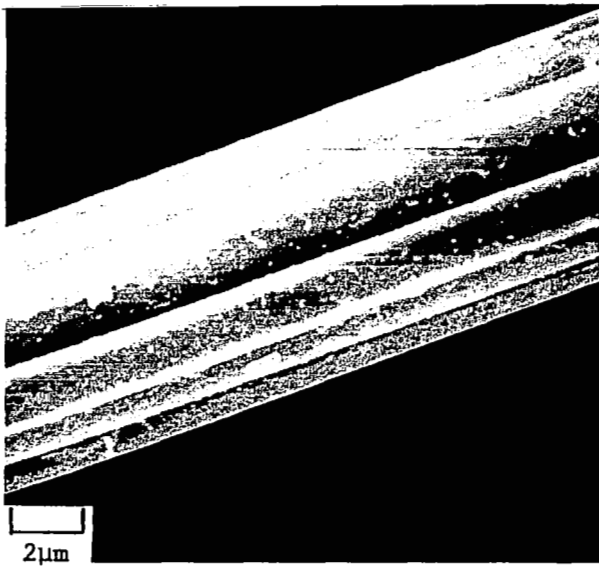
(a)   (b)

Fig. C3.   Typical example of nodules on an otherwise uniformly TiC-coated fiber
           surface.   (a) Specimen image.   (b) Ti x-ray image (Run 4D).

(a)   (b)

Fig. C4.   Example of (a) severe cracking in TiC coat on graphite fibers and
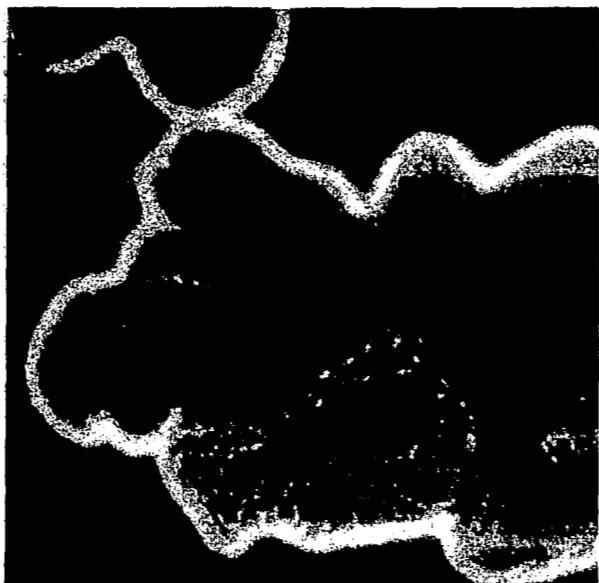   (b) separation of coat from surface of fibers (Run 5A).

Fig. C5. Polished cross sections of TiC-coated graphite fibers, showing typical welding together of fibers (Run 4A).

Fig. C6. Polished cross sections of TiC-coated graphite fibers, showing nonuniform distribution of TiC from one fiber to another and on individual fibers (Run 8FF).

APPENDIX D

FLEXURE TESTING

Aluminum-graphite composite flexure bars were tested in a four-point loading fixture, with 1.59-mm-diam support and load pins located at major and minor spans of 25.4 mm (L) and 12.5 mm (ℓ), respectively. The fixture, shown schematically in Fig. D1, was equipped with a direct current differential transducer which was used to measure the deflection of the sample during testing. Deflection was measured relative to the minor span on the flexure specimen. The load was applied with a tensile testing machine at a cross-head speed of 1.27 mm/min. Stresses (σ) and strains (ε) were calculated from the following standard beam equations:

$$\sigma = \frac{3PL}{4wt^2} \quad \text{and} \quad \varepsilon = \frac{4t\delta}{\ell^2} \quad ,$$

where P = applied load, w = specimen width, t = specimen thickness, δ = deflection, L = major span of the fixture and ℓ = minor span. The rule-of-mixtures (ROM) strength (σ_c) was calculated from the expression

$$\sigma_c = v_f \sigma_f + v_a \sigma_a \quad ,$$

where v_f and v_a are the volume fractions of the fibers and alloy matrix, respectively, in the composite, σ_f is the strength of the individual fibers, and σ_a is the stress in the aluminum alloy corresponding to the strain at which fracture occurred in the composite. The volume fraction of fibers (v_f) in the composite was computed with the assumption that the individual fibers were round in cross section with a uniform diameter of 6.5 μm.[4] The individual fiber strengths were computed from the expression

$$\sigma_f = \frac{S_f}{S_o} (\sigma_o) \quad ,$$

where σ_o = 2.172 GPa (315 x 10^6 psi), the manufacturer's strength for individual Thornel 50 fibers, and S_f and S_o = tensile breaking loads for single-ply samples of TiC-coated fiber yarns and Thornel 50, respectively. σ_a was taken from the flexure stress-strain curve shown in Fig. D2, which was determined from tests on as-cast bars of Al-13% Si matrix alloy. The values given in Fig. D2 were computed using the above standard beam equations, which assume elastic behavior. Therefore, values beyond the elastic limit do not necessarily represent the actual stress-strain behavior of this material. However, the values given in the figure should be adequate for the comparison and computation of composite ROM strengths given here.

An example of a typical load-deflection curve of an aluminum-graphite composite flexure bar is shown in Fig. D3, and the sample as it appeared after
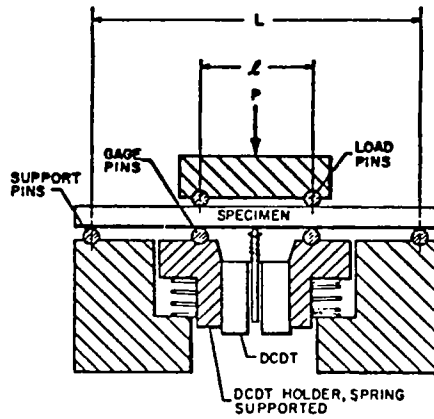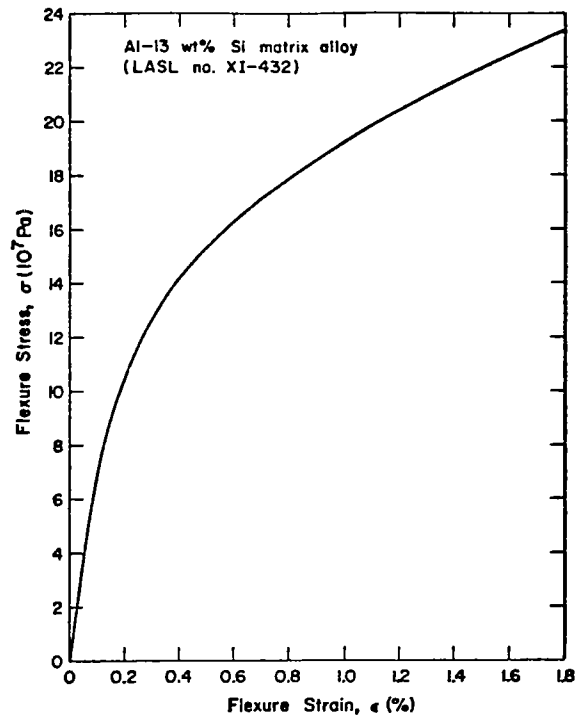
Fig. D1. Schematic of flexure testing fixture.

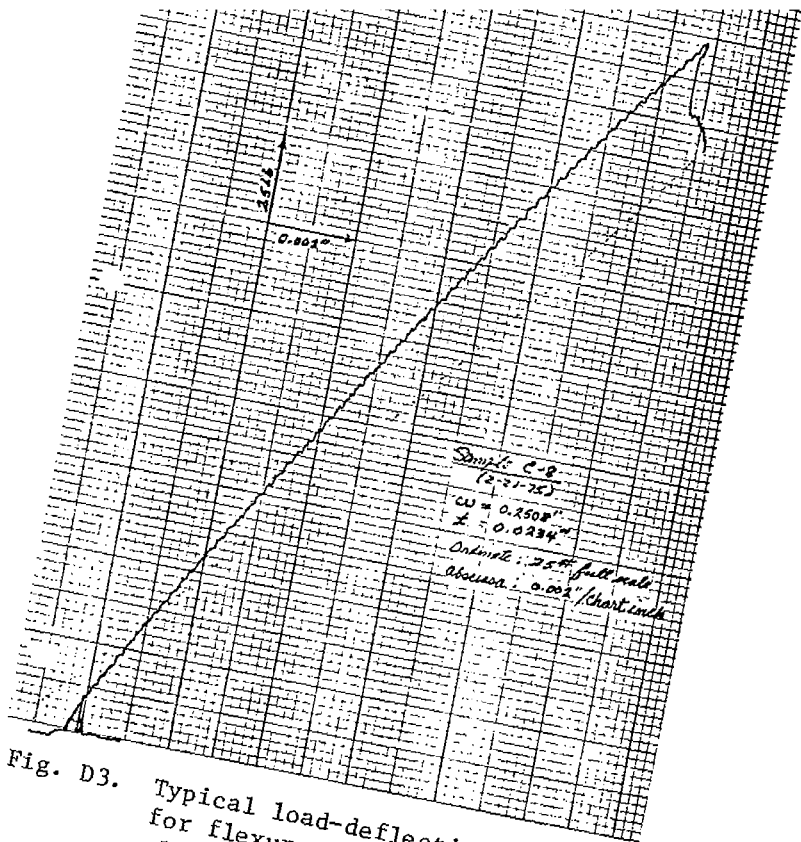Fig. D2. Flexure stress-strain curve for as-cast bars of Al-13 wt% Si matrix alloy.

Fig. D3. Typical load-deflection curve for flexure test of a graphite-aluminum composite.
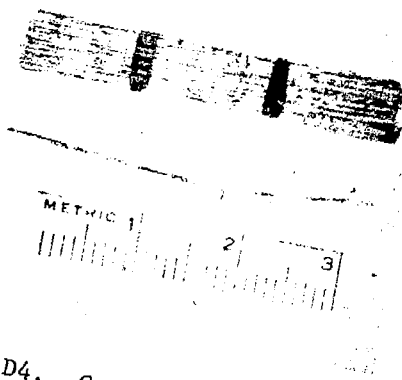

Fig. D4. Compacted bar of Al-infiltrated Thornel 50 fibers after flexure testing. Top view (above) and edge view (below).

testing in Fig. D4. The dark ink marks on the sample, in the top view, indicate the position of the load pins on the compression face of the sample. The failure region is clearly shown in the edge view (bottom) between the pins near the left-hand mark. The maximum strength shown on the load-deflection curve (Fig. D3) apparently corresponds to the point at which the fibers in the composite begin to break. The corresponding strain, however, is much less than that necessary to initiate fracture in the ductile aluminum matrix. This is shown by the fact that the sample did not separate into two pieces during testing.

REFERENCES

1. Imprescia, R. J., Levinson, L. S., Reiswig, R. D., Wallace, T. C., and Williams, J. M., "Carbide Coated Fibers in Graphite-Aluminum Composites, Progress Report No. 1: Sept. 1, 1973 – Jan. 31, 1974," NASA CR-2533, August 1975.

2. Imprescia, R. J., Levinson, L. S., Reiswig, R. D., Wallace, T. C., and Williams, J. M., "Carbide Coated Fibers in Graphite-Aluminum Composites, Progress Report No. 2: February 1 – July 31, 1974," NASA CR-2566, July 1975.

3. Imprescia, R. J., Levinson, L. S., Reiswig, R. D., Wallace, T. C., and Williams, J. M., "Carbide Coated Fibers in Graphite-Aluminum Composites, Progress Report No. 3: August 1 – December 31, 1974," NASA CR-2601, October 1975.

4. B. L. Butler, "Application of Engineering Data on Carbon Fibers to Carbon-Carbon Composites," Sandia Laboratories Report No. SLA-73-0385B, September 1973.